Acta Geologica Sinica (English Edition), 2023, 97(1): 288–308

Deciphering the Origin of Abiotic Organic Compounds on Earth: Review and Future Prospects

WANG Chao[1, 2], TAO Renbiao[2], Jesse B. WALTERS[3], REN Tianshi[1, 2], NAN Jingbo[4] and ZHANG Lifei[1, *]

[1] *MOE Key Laboratory of Orogenic Belts and Crustal Evolution, School of Earth and Space Sciences, Peking University, Beijing 100871, China*
[2] *Center for High Pressure Science and Technology Advanced Research (HPSTAR), Beijing 100094, China*
[3] *Institut für Geowissenschaften, Goethe-Universität Frankfurt, Frankfurt am Main 60438, Germany*
[4] *Department of Ocean Science and Engineering, Southern University of Science and Technology, Shenzhen 518055, China*

Abstract: The geologic production of abiotic organic compounds has been the subject of increasing scientific attention due to their use in the global carbon flux balance, by chemosynthetic biological communities, and for energy resources. Extensive analysis of methane (CH_4) and other organics in diverse geologic settings, combined with thermodynamic modelings and laboratory simulations, have yielded insights into the distribution of specific abiotic organic molecules on Earth and the favorable conditions and pathways under which they form. This updated and comprehensive review summarizes published results of petrological, thermodynamic, and experimental investigations of possible pathways for the formation of particular species of abiotic simple hydrocarbon molecules such as CH_4, and of complex hydrocarbon systems, e.g., long-chain hydrocarbons and even solid carbonaceous matters, in various geologic processes, distinguished into three classes: (1) pre- to early planetary processes; (2) mantle and magmatic processes; and (3) the gas/water-rock reaction processes in low-pressure ultramafic rock and high-pressure subduction zone systems. We not only emphasize how organics are abiotically synthesized but also explore the role or changes of organics in evolutionary geological environments after synthesis, such as phase transitions or organic-mineral interactions. Correspondingly, there is an urgent need to explore the diversity of abiotic organic compounds prevailing on Earth.

Key words: abiotic hydrocarbons, high *P-T*, methane, abiotic solid organic compounds, deep carbon cycle

Citation: Wang et al., 2023. Deciphering the Origin of Abiotic Organic Compounds on Earth: Review and Future Prospects. Acta Geologica Sinica (English Edition), 97(1): 288–308. DOI: 10.1111/1755-6724.15045

1 Introduction

The basic chemical ingredients for organic life are carbon–hydrogen (C–H) molecules. Thus, habitable environments require organic molecules, as well as liquid water, a pre-requisite that is met throughout the solar system. Liquid water has existed transiently on some planetary bodies such as Mars and persistently as oceans on others, e.g., Earth, Enceladus, and Titan. Methane (CH_4) has been also observed in many places besides Earth, from the dusty plains of Mars to the great lakes of the Saturnian Moon Titan and the glacial wonderland of Pluto (Glein and Zolotov, 2020). Indeed, organic compounds, such as CH_4, can be produced abiotically and their existence may shed light on the habitability of the solar system. Early life on Earth may have been generated and/or sustained by abiotic organic compounds in extreme environments (Brovarone et al., 2020). These environments are potential targets for extraterrestrial life, as well as for the discovery of new chemosynthetic biological communities on Earth (e.g., Ménez, 2020).

Organic compounds are usually reducing substances, e.g., CH_4, and can be produced in a variety of settings, including interstellar environments in solar nebulae to the deep Earth. Indeed, such molecules may even play a role in regulating Earth's redox evolution under high-temperature (HT) and high-pressure (HP) conditions in subduction zones and the deep mantle (e.g., Sverjensky et al., 2014; Brovarone et al., 2017; 2020; Walters et al., 2020; Debret et al., 2022; Wang et al., 2022). Some studies have even proposed that deep abiotic hydrocarbons represent potentially untapped energy resources that have not yet been targeted by the oil and gas industry (Kutcherov and Krayushkin, 2010; Truche et al., 2020).

In line with other authors (cf. McCollom and Seewald 2007; Etiope and Sherwood Lollar, 2013; Reeves and Fiebig, 2020), we use 'abiotic' to describe organic compounds formed by purely non-biological, i.e., abiotic or abiogenic synthesis reactions: reactions not involving complex organic precursors or biological activity, e.g., the inorganic reduction of oxidized carbon. Identification of abiotic CH_4 and co-occurring light hydrocarbons (C_2–C_4) has been exhaustively conducted in the field of petroleum and gas science, see reviews in Etiope and Sherwood Lollar (2013) and Reeves and Fiebig (2020) for further information. As a complement, we review here the new

* Corresponding author. E-mail: lfzhang@pku.edu.cn

breakthroughs in the identification of abiotic organics by petrologists in recent years, which have been aided by the development of in situ high-resolution imaging techniques, e.g., synchrotron-coupled deep-ultraviolet (S-DUV), photo-induced force microscopy (PiFM), and others.

Moreover, this paper is an updated and comprehensive review that summarizes published results of petrological, thermodynamic, and experimental investigations of possible pathways for the formation of particular species of abiotic simple hydrocarbon molecules (e.g., CH_4), complex hydrocarbon molecules (e.g., long-chain hydrocarbons) and solid carbonaceous matter (CM, solid organic compounds as independent phases or adsorbed on minerals) in various geologic systems. Here we divide these systems into 3 main coherent classes: (1) pre- to early planetary process; (2) mantle and magmatic process; (3) gas/water-rock reaction processes in low-pressure ultramafic rock system (crustal level) to high-pressure subduction zone systems (crust-mantle interaction level). In response to these studies, we further highlight gaps in the existing body of knowledge and suggest some key future research directions. Additionally, we not only emphasize how organics are abiotically synthesized but also the role organics play in geological environments after synthesis, such as phase transitions or organic-mineral interactions. The diversity of abiotic organic compounds prevailing in the deep earth, such as in subduction zone systems, is only beginning to be explored.

2 Pre- to Early Planetary Process

Carbon (C) is the 4th most abundant element in the Universe and highly complex organic compounds involving this element have been discovered on objects from the solar system and more distant galaxies (Kwok, 2009). Space remote sensing techniques, e.g., space infrared spectroscopy, have identified more than 150 molecules with stretching and bending modes of compounds with aromatic and aliphatic structures (Kwok, 2009, 2015). For research in astronomy, one of the most definite and surprising knowledge of molecular synthesis comes from circumstellar envelopes of evolved stars, from the asymptotic giant branch (AGB) stars to proto-planetary nebulae to planetary nebulae, over very short ($\sim 10^3$ yr) time scales. Specifically, carbon is synthesized in the core of AGB stars by nucleosynthesis and then dredged up to the star surface, and, subsequently, new C-bearing molecules with increasing complexity are detected through infrared and millimeter-wave spectroscopy in the stellar winds ejected from these stars (Kwok, 2015). By these processes, simple molecules, such as acetylene (C_2H_2), CN chains (HCN, HC_3N, HC_5N), and rings (C_3H_2), are formed at first in the stellar winds of AGB stars, followed by the formation of di-acetylene, tri-acetylene, and the first aromatic molecule, benzene, in the proto-planetary nebula stage. Finally, in the young planetary nebula, nanoparticles of mixed aromatic-aliphatic structures (MAON, Kwok and Zhang, 2011, 2013; Figs. 1a–b) are synthesized, which contain

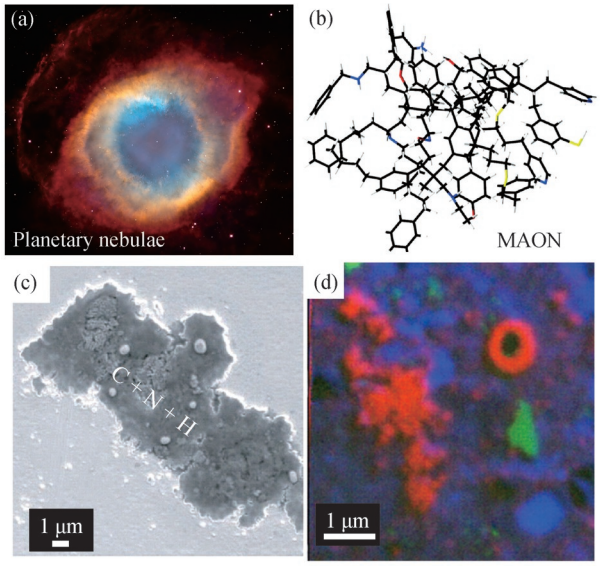

Fig. 1. Solid organic matters produced during the pre- to early planetary process.
(a) An image of a planetary nebula photographed by Hubble Space Telescope (from NASA Hubble material—https://apod.nasa.gov/) and (b) a 3D illustration of a possible partial structure of a MAON particle detected in a planetary nebula (from Kwok and Zhang, 2017; reprinted by permission from Springer Nature, copyright). Carbon atoms are represented in black, hydrogen in light gray, sulfur in yellow, oxygen in red and nitrogen in blue. There are 101 C, 120 H, 14 O, 4 N, and 4 S atoms in this example; (c) SEI image of IOMs containing C–N–H elements in Tagish Lake chondrites (from Busemann et al., 2006; reprinted with permission from AAAS); (d) A scanning transmission X-ray map of carbon (red), iron (blue), and calcium (green) concentration of solid organic micro- and nanospheres in Murchison carbonaceous chondrite (MUR). And corresponding in-situ C-XANES and ^{13}C CPMAS NMR spectral analysis from Cody et al. (2011) reveal the presence of olefinic and aromatic carbon, ene-ketone, enol, and carboxyl carbon, alcohols, methine carbon in these IOMs.

impurities such as O, S, and N. In the laboratory, by introducing H into graphite (sp^2) and diamond (sp^3), a variety of amorphous C–H alloys can be synthesized. Geometric structures with different long- and short-range order can be created by varying the sp^2/sp^3 hybridization ratios. Considering the widespread presence of carbon and hydrogen, such complex amorphous organic solids may be widely present in space, because the infrared spectra of MAON from planetary nebulae resemble these amorphous carbonaceous materials (Dischler et al., 1983; Kwok, 2015).

In the past, direct chemical analysis of extraterrestrial material was conducted on meteorite samples. However, modern spacecraft have given us the ability to send instruments to solar system objects for in situ measurements and to return rock samples to Earth for further analysis. Such missions will allow us to better understand the presence or absence of abiotic organic matter in our solar system (Kwok, 2017, 2019). With the former, the first evidence for the existence of extraterrestrial organics came from carbonaceous chondrites (Hayes, 1967), a rare category of meteorites that are thought to be the most pristine (McSween, 1979). By using different solvents, various soluble components in meteorites can be extracted and analyzed by gas

chromatography (GC), which yields carboxylic acids, sulfonic and phosphonic acids, amino acids, aromatic hydrocarbons, etc. However, insoluble organic matter (IOM) is the major constituent (70%–90%) of abiotic organics in extraterrestrial materials (Naraoka, 2014; Fig. 1c). In the past, the IOM was referred to as kerogen-like material, cf. kerogen, a solvent-insoluble organic matter in terrestrial rocks, or macromolecular organic matter. The H/C ratio of chondritic IOM varies from <0.1 to 0.7 and the more metamorphosed meteorites have lower H/C ratios, but the average elemental abundance of IOM can be represented by the formula $C_{100}H_{46}N_{10}O_{15}S_{4.5}$ (Pizzarello and Shock, 2010). These solids are amorphous in structure and consist of small aromatic rings connected by short aliphatic chains mixed with other heavy elements, such as O, N and S, as revealed by ^{13}C-nuclear magnetic resonance (NMR) and X-ray absorption spectroscopy (XANES) studies (Fig. 1d; Cody et al., 2011). There are also reports of abiotic organics in our solar system from sources other than meteorites. These include: (1) the mass spectrometer aboard Rosetta's Philae lander has detected CH_3NCO, CH_3COCH_3, C_2H_5CHO, and CH_3CONH_2 on the surface of comet 67P/Churyumov-Gerasimenko (Goesmann et al., 2015); (2) macromolecular compounds similar to meteoritic IOM are found in cometary dust (Fray et al., 2016), suggesting both aromatic and aliphatic materials exist; and (3) thiophenic, aromatic, and aliphatic compounds have been identified in drilled samples from the Gale crater on Mars by in situ heating to 860°C for gas chromatography–mass spectrometry (GC–MS) analysis onboard NASA's Curiosity rover, which have been traced to kerogen-like precursor materials (Eigenbrode et al., 2018). Compared with terrestrial planets, gas giants and ice giants, such as Jupiter, and their moons are more abundant in abiotic organic molecules. For example, Postberg et al. (2018) detected organic molecules in plumes from Saturn's 6th moon Enceladus, indicating the presence of a large reservoir of complex macromolecular organics in the subsurface oceans. While the surface of Enceladus is dominated by H_2O-ice, below the ice shell is a global ocean of cold liquid water (~70 bar), beneath which is a deep ultramafic rock core that is expected to be in contact with the liquid ocean (Glein and Zolotov, 2020; Truche et al., 2020). Serpentinization processes would probably occur in this environment with reactions such as 3FeO (in silicates) + H_2O (liq) → Fe_3O_4 (magnetite) + H_2 (↑). Carbon, if present, will, with H_2, produce organic C–H molecules such as CH_4, as has been observed during terrestrial serpentinization (Sherwood Lollar et al., 2002, 2014; Andreani and Ménez, 2019). The low density of Enceladus's core (~2.4 g·cm^{-3}) is consistent with the presence of phyllosilicates such as serpentine. In other examples, Saturn's moon Titan (the second largest moon in the solar system) was found to have large lakes of liquid CH_4 and ethane (C_2H_6), as well as organic particles in the surface dunes and its atmosphere (~1.5 bar, with almost no oxygen but dominated by N_2 and CH_4), as detected by infrared spectroscopy (Kim et al., 2011; Tobie et al., 2012; Le Gall et al., 2016). Photochemical models predict that the CH_4 in Titan's atmosphere cannot be sustained for more than ~30 My (Thompson et al., 2022), thus the existence of a modern CH_4 atmosphere comes from the recharge of liquid hydrocarbons in its subsurface ocean and methane hydrates in the crust (Tobie et al., 2012). Furthermore, photochemically induced ionization, by UV light and other energetic particles, of CH_4 and N_2 can initiate a series of chemical reactions leading to the synthesis of more complex organic compounds. Some reddened and darkened areas on Pluto's surface are thought to be caused by haze from photochemical reactions (Glein and Zolotov, 2020).

Since almost all stars go through the AGB–pre-planetary nebulae–planetary nebulae stage, significant organic molecules may be produced and distributed all over the galaxy (Kwok, 2004). The detection of pre-solar grains in meteorites suggests that material from AGB stars can survive the journey through the interstellar medium and reach the solar system (Kwok, 2017). Since the Earth was formed from planetesimals, it is possible that the Earth also inherited primordial organic molecules ejected by stars. As the Earth condensed from a hot molten state after a period of coalescence of smaller bodies through accretion, the high temperatures and collisional shock would make it very difficult for simple hydrocarbons to survive. However, solid organic compounds, e.g., hydrogenated graphitic C (Yang et al., 2021) are stable to higher pressures and temperatures since simple organics, e.g., CH_4, *n*-hexane, tend to undergo dehydropolymerization to produce immobile solid carbon species as *P* and *T* increase (see review below), increasing the chances that primordial hydrocarbons would have survived during Earth's formation. One may ask whether there are any reserves of primordial organic molecules in the deep Earth, an area which will benefit from the study of condensed carbonaceous matter (CCM) in the future.

Due to the difficulty of in situ observation and the scarcity of samples, in most cases, research based on astronomical or meteorite studies can only make estimates on the presence and speciation of C-based molecules. However, future international space missions, such as ExoMars, Juice, and Dragonfly, will attempt to illuminate the 'organic solar system' and the role played by possible extraterrestrial life. In time, the link between geochemical phenomena and the creation of habitable worlds will ultimately be revealed, from our cosmic backyard to the far frontiers of space (Glein and Zolotov, 2020).

3 Mantle and Magmatic Processes

3.1 Observations in Earth's mantle

Dmitri Mendele'ev (1877), father of the periodic table of the elements, was the first to suggest that abiotic organic molecules might be present in the Earth's mantle. He reacted H_2O with metallic carbides to form acetylene (C_2H_2), which then condensed to heavy hydrocarbon molecules, and thus he postulated that similar reactions may occur in the deep Earth. However, carbides are unlikely to be abundant enough in the mantle for such reactions to be a significant source of abiotic organic molecules (Etiope and Sherwood Lollar, 2013). Primary organic molecules, mainly CH_4, in the deep mantle are found in exhumed diamonds and mantle-plume volcanic

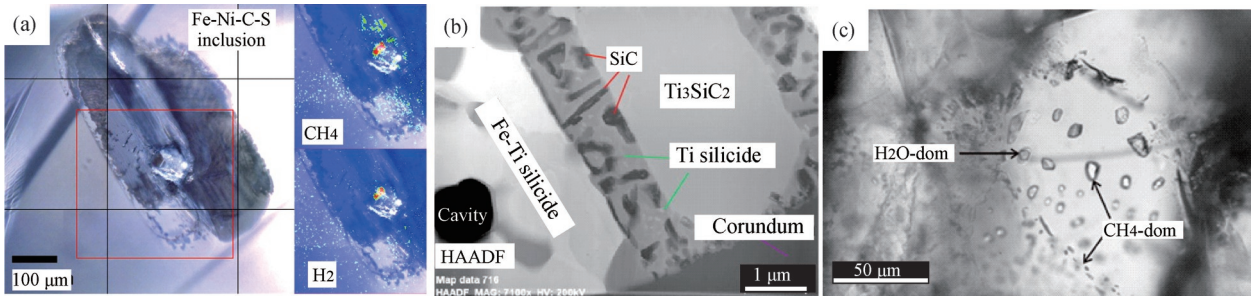

Fig. 2. Hydrocarbon-bearing fluid/melt inclusions observed in natural samples associated with mantle and magmatic processes. (a) CH_4 and H_2 concentrated in a Fe–Ni–C–S melt inclusion in CLIPPIR diamonds (from Smith et al., 2016; reprinted with permission from AAAS); (b) inclusions in SiC from the Mt Carmel basaltic pyroclastic rocks, Israel (from Huang et al., 2020; reprinted with permission from Elsevier, copyright); (c) H_2O-dominant inclusions in trails with CH_4-dominant inclusions in eudialyte from alkaline igneous rocks in the Lovozero complex, Russia (from Potter et al., 2004; reprinted with permission from Elsevier, copyright).

rocks. Smith et al. (2016, 2018) reported some Fe–Ni–C–S melt inclusions in large diamonds from Earth's lower mantle and found CH_4–H_2 Raman bands within these melt phases (Fig. 2a); therefore, it was proposed that the lower mantle is a reducing environment, saturated with iron and nickel metals, where diamond is precipitated from an HP Fe–Ni–C–S melt. Alternatively, hydrogen may have a high solubility in such melts and any CH_4 is the result of the reaction of diamond and hydrogen. Similarly, Huang et al. (2020) found Si–Fe–Ti–C metallic melt inclusions in moissanite (SiC) in volcanic eruptive basaltic rocks and kimberlites from a mantle plume (Fig. 2b), and the volatiles released from the moissanite grains were H_2 + CH_4 ± CO_2 ± CO, identified by GC. Huang et al. (2020) therefore proposed that SiC can directly crystallize from reduced metallic melts in a low oxygen fugacity (fO_2)-controlled upper mantle environment containing H_2 and CH_4. Such petrological observations tell us that, at low fO_2 thermodynamic conditions in a metal-saturated mantle, the fluid/melt C–H(–O) species will mainly exist in the form of H_2 and CH_4. However, to date, all reported abiotic organic molecules are in the form of low-density gases/fluids, C_1–C_4 mainly CH_4, and solid organic compounds have not been observed. One exception may be from Garanin et al. (2011), whom claim to have found polyaromatic hydrocarbons (PAHs) in majoritic garnets from the highly diamondiferous Mir kimberlite pipe in Russia. In this case, the polyphase fluid inclusions, PAHs, water solutions, and CO_2, confirmed by in situ Raman and IR spectroscopy, are uniformly distributed within the majoritic garnets and are not confined to the cracks, which are regarded as the features of primary inclusions and indicate the hydrocarbon-specific character of the fluids that participate in the processes of deep mineral formation.

Thermodynamic model predictions and HP-HT experiments have also provided constraints on detailed C–H species in the mantle. Early work was carried out by the Ukrainian petroleum scientist Alexander Chekalyuk (1971), who conducted basic thermodynamic studies on complex hydrocarbons under extreme thermobaric conditions. The starting materials were mainly alkanes, alkenes, alkynes, naphthenes, aromatics, and their isomers. Chekalyuk's (1971) calculations show that at relatively low temperatures, even at pressures of several GPas, CH_4 will always dominate the system at equilibrium, implying that pressure alone is insufficient to convert CH_4 into heavier hydrocarbons. As temperature increases, denser saturated alkanes are formed, followed by unsaturated alkanes, cyclic and aromatic compounds. The experimental conditions of 5–8 GPa and 1100–1700°C correspond to depths of 150–220 km, where, at the highest *P-T*, the system is dominated by aromatics. Kenney et al. (2002) calculated the stability of C_1–C_{20} hydrocarbons at different *P-T*; their results showed that low-*P* conditions at fixed high-*T* (1000 K) stabilizes CH_4 and only at pressures greater than 2.5 GPa is CH_4 converted to heavier alkanes (Fig. 3a). Lobanov et al. (2013) experimentally constructed phase diagrams for CH_4 at *P-T* conditions up to 80 GPa and 2000 K using a laser- and external-heated diamond anvil cell (DAC) apparatus. The melting curve of CH_4 was determined first as the experimental temperature increased, followed by the stability of H_2 and C^0 at > 1200 K, and finally the presence of heavier alkanes and unsaturated hydrocarbons formed at >1500 K conditions (Fig. 3c). Therefore, the C–H fluids will evolve towards heavy hydrocarbons in the deep earth. In turn, reduced deep mantle fluids are expected to convert to CH_4 and precipitate diamond/graphite as they ascend to the upper mantle or crust. This is a key example of a phase transition between different abiotic organic species that occurs in the simple C–H system.

Early thermodynamic models or experimental simulations only consider organic molecular phases and do not involve any solid crystalline phases, dissolved ions, or water-organic interactions. Zhang and Duan (2009) developed an equation of state for mixed C–O–H fluids that can be applied to thermodynamic calculations involving multi-fluid and multi-solid species to predict the abundance of O_2, H_2O, CO_2, CH_4, H_2, CO, and C_2H_6 at HT and HP up to 10 GPa, 2573 K. While previous equations of state had been developed for mixed C–O–H fluids, these were primarily applicable to crustal conditions (e.g., Holland and Powell, 1991; Saxena and Fei, 1987). Zhang and Duan (2009) calculated the low fO_2 conditions favorable for hydrocarbon formation in the upper mantle and found that CH_4 abundance increases with depth, whereas CO_2 has the opposite trend. Going further, Sverjensky et al. (2014) developed the Deep Earth Water Model (DEW) for thermodynamic calculations, up to 6 GPa, 1200°C, involving solid minerals, mixed solvent

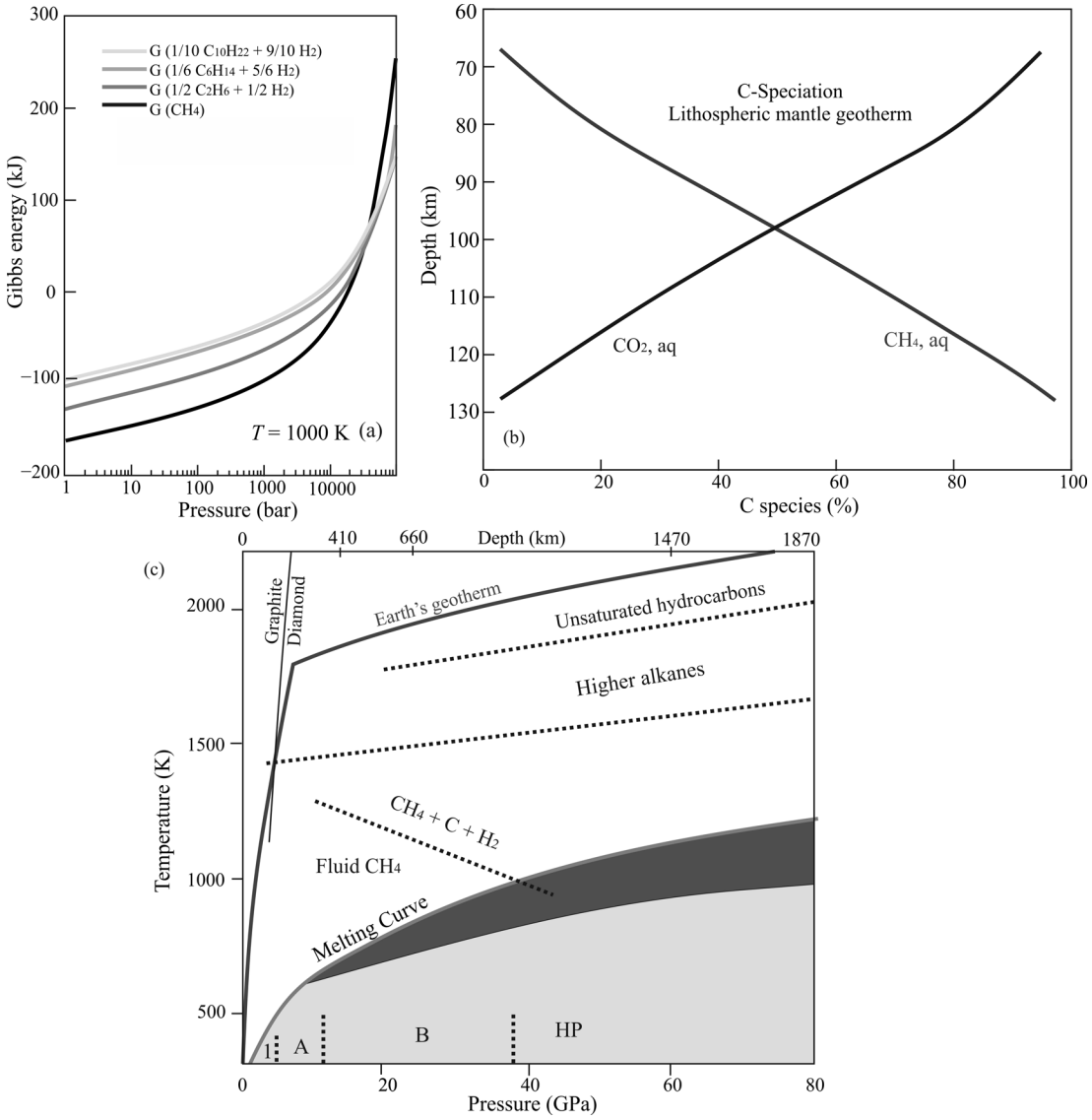

Fig. 3. C–H species in the mantle constrained by thermodynamic models and high-pressure experimental simulations.
(a) Gibbs energies of CH_4 and of the C–H system at 1000 K (modified after Kenney et al., 2002; copyright (2002) National Academy of Sciences, U.S.A.); (b) aqueous C-speciation in peridotitic fluid containing 1.0 m C and Cl predicted by the DEW model (modified after Sverjensky et al., 2014; reprinted by permission from Springer Nature, copyright); (c) phase diagram of C–H system with CH_4 as a starting material (modified after Lobanov et al., 2013 and reprinted by permission from Springer Nature, copyright). The thick solid line represents the upper limit of the melting curve of CH_4; the filled light grey area shows a solid CH_4 region and solid phases (1, A, B, HP) and boundaries between are marked; the filled dark grey area represents the CH_4 melting zone according to laser heating (LH) DAC experiments because of temperature uncertainties; graphite-diamond equilibrium and the Earth's geotherm lines are, respectively, shown for comparison. Thick dashed lines summarize data for chemical reactivity.

species, neutral solute molecules, and charged ions to predict changes in fluid species. Sverjensky et al. (2014) and Sverjensky (2020) predicted that abundant and diverse aqueous abiotic organic and inorganic C species will emerge at high pressures: at crustal pressures and at temperatures greater than about 500° C, the expected thermodynamic equilibrium speciation of C is CO_2(aq), CH_4(aq), HCO_3^-, CO_3^{2-}, whereas at high *P-T* (5 GPa, 600° C) CH_3COO^- and CH_3COOH(aq) are predicted. Aqueous speciation calculations along a representative mantle geotherm show that at a depth of about 100 km, the fluid is predicted to transition from CO_2-dominated to CH_4-dominated (Fig. 3b), consistent with Zhang and Duan (2009). Therefore, if a source of C and fluids is available, it is possible that CH_4, C_2H_6, and other hydrocarbons are present within the mantle.

3.2 C–H–O speciation in magmatic systems

The average calculated fO_2 of mid-ocean ridge basalt (MORB) is +0.1 relative to a fayalite–quartz–magnetite buffer (FMQ) (see review in Berry and O'Neill, 2021), consistent with CO_2-dominant fluids at magmatic temperatures. Magmas from other settings, such as volcanic arcs, are also equally or even more oxidized relative to MORB (see review in Cottrell et al., 2021). Indeed, Wogan et al. (2020) predicted the speciation of C–H–O fluids during magma cooling and degassing progress by thermodynamic calculation (in the range of 1–1000 bar,

1000–2000 K, FMQ+2–FMQ−5): CH_4 can become the dominant species in the system only under low-*T* and high -*P* conditions at low oxygen fugacity. While abiotic organic molecules are not stable in high *T*-low *P* magmatic systems, they may be generated during cooling and re-equilibration. CH_4 can be generated via the reaction $CO_2 + 2H_2O = CH_4 + 2O_2$, as this equilibrium re-adjusts to temperatures below 500°C, which has been proposed to explain the presence of CH_4 in magmatic gases and mineral inclusions (see review in Etiope and Sherwood Lollar, 2013). For example, Kelley (1996) conducted a Raman spectroscopy study of fresh gabbro from the mid-Indian ocean ridge and found CH_4–H_2–C^0–H_2O fluid inclusions in feldspar. Combined with phase equilibrium simulations, Kelley (1996) proposed that CH_4 formed by re-equilibration of magmatic volatiles at low fO_2 conditions (FMQ−3) during cooling to 500–600° C, resulting in secondary CH_4-bearing fluid inclusions, or by post-entrapment modification of primary magmatic fluid inclusions. Fischer–Tropsch (F–T) type reactions during postmagmatic alteration may also occur; this process involves reactions between a CO_2-rich fluid and H_2 generated during alteration, specifically involving Fe-rich minerals as a redox couple (e.g., $Fe^{2+}O + H_2O \rightarrow Fe^{3+}{}_2O_3 + H_2$; H_2+CO/CO_2 → CxHy + H_2O). For example, Potter et al. (2004) found secondary fluid inclusions of CH_4 (accompanying ethane, propane, and hydrogen) in neolite and nepheline of the alkaline igneous rocks in the Lovozero complex, NW Russia (Fig. 2c). Based on the homogenization temperatures and densities of the fluid inclusions, Potter et al. (2004) estimated that the formation temperature of CH_4 was less than 400°C at pressures of < 2 kbar. The mass spectrometry (MS) analysis of C isotopes is consistent with an abiotic origin, e.g., $\delta^{13}C_{CH4}$ falls between −15.7‰ and −3.2‰, and consistent with the following reactions: $Na_3Fe_4^{2+}Fe^{3+}Si_8O_{22}(OH)_2$ (arfvedsonite) + $2NaAlSiO_4$ (nepheline) + $4H_2O$ = $5NaFe^{3+}Si_2O_6$ (aegirine) + $2Al(OH)_3$ + $2H_2$; $(2n+1)H_2 + nCO \rightarrow C_nH_{2n+2} + nH_2O$ or $(3n+1)H_2 + nCO_2 \rightarrow C_nH_{2n+2} + 2nH_2O$. However, low-*T* alteration of mafic to ultramafic rocks by external fluids is likely a larger source of abiotic CH_4, as detailed in the next section.

In conclusion, abiotic hydrocarbons are not anticipated to be generated at magmatic temperatures, but organic molecules may form during cooling and re-equilibration of magmatic-hydrothermal fluids under suitable *P-T-*fO_2 conditions. Given that the fO_2 conditions of magmas do not stabilize CH_4, the CO_2/CH_4 ratio of fumarolic gases is sensitive to the gas source, increases in the CO_2/CH_4 indicate a transition from low fO_2 hydrothermal-dominant processes to higher-fO_2 magmatic processes (Chiodini, 2009).

4 Gas/Water-Rock Interaction Process

4.1 Low-pressure ultramafic rock system (crustal level)

4.1.1 Natural observations

(1) Light-hydrocarbons

Most previous studies hypothesized that the formation of light-hydrocarbon (e.g., C_1–C_4) is associated with the serpentinization of ultramafic rocks (Andreani and Ménez, 2019). Under the umbrella term 'serpentinization', a series of reactions convert inorganic carbon, such as CO_2 or CO, into organic compounds via abiotic redox reactions. First proposed by Berndt et al. (1996), H_2 is produced from water through the oxidation of igneous Fe^{2+}-bearing minerals (e.g., olivine) to form secondary Fe^{3+}-bearing minerals, mainly magnetite and minor Fe^{3+} in serpentine. Abiotic hydrocarbons (C_xH_y) are then produced by the F–T reaction between H_2 and oxidized carbon in gases/fluids, e.g., HCO_3^-, CO_3^{2-}, or minerals, e.g., carbonates (Berndt et al., 1996). The abiotic light hydrocarbons formed by this process can be CH_4 or volatile organic acids, e.g., formic acid, the latter of which has been detected in hydrothermal fluids (see below).

Abundant abiotic CH_4 and H_2 have been detected in seafloor alkaline hydrothermal vents, such as the Rainbow and Lost City field in the Mid-Atlantic Ridge (Charlou et al., 2002; Kelley et al., 2005). These hydrothermal circulation cells drive serpentinization at mid-ocean ridges, where fluids are channeled along fractures and fault planes between down-dropped blocks. Serpentinization is particularly prevalent at slow-spreading ridges and oceanic core complexes, where peridotite is exposed at or near the seafloor (e.g., Mével, 2003; Ildefonse et al., 2007). Similarly, subaeral abiotic CH_4- and H_2-rich fluids, such as the well-known 'Eternal Fire', burning H_2–CH_4 gas flow on the Chimaera ophiolite, Turkey (Vacquand et al., 2018), CH_4-rich gas deposits found in mining sites in the Canadian and Fennoscandian shields (Sherwood Lollar et al., 1993), and H_2–CH_4 gas collected in water springs on the Semail ophiolite of Oman (Vacquand et al., 2018), also result from the interaction of ultramafic rocks with groundwater in deep subsurface fault systems.

On the basis of stable isotopic (Xe–He–Ne–Ar) analysis, Holland et al. (2013) speculated that deep fracture fluids rich in CH_4, C_2H_6, H_2, He, etc., in Precambrian shields could be preserved in the crust for billions of years. C–H isotopic evidence (^{13}C isotopic depletion and ^2H enrichment between C_1 and C_2) supports an abiotic origin for these fluids (Sherwood Lollar et al., 2002, 2014). Serpentinization and radiolysis of H_2O are thought to work together to provide the H_2 required for hydrocarbon synthesis in these fluids. In radiolysis, K, Th, and U in minerals decay to generate α, β, and γ radiation, which breaks apart the H–O bond of water and generates hydrogen radicals (H•) and hydroxyl radicals (OH•), which can then recombine to generate H_2 (Sherwood Lollar et al., 2014; Klein et al., 2020).

(2) Solid abiotic organic compounds

In addition to the abiotic synthesis of low-molecular-weight organic compounds, in situ highly temporal/spatial resolved spectroscopic characterization techniques have allowed for the identification and imaging of condensed carbonaceous matter (CCM), as well as the textural relationship of these compounds with their mineral parageneses (Andreani and Ménez, 2019). Recently, abiotic macromolecular CCMs (solid organic compounds) have been found in abyssal serpentinites and high-P serpentinite (at < 0.6 GPa) (Ménez et al., 2018a, b; Sforna et al., 2018; Nan et al., 2021; Debret et al., 2022),

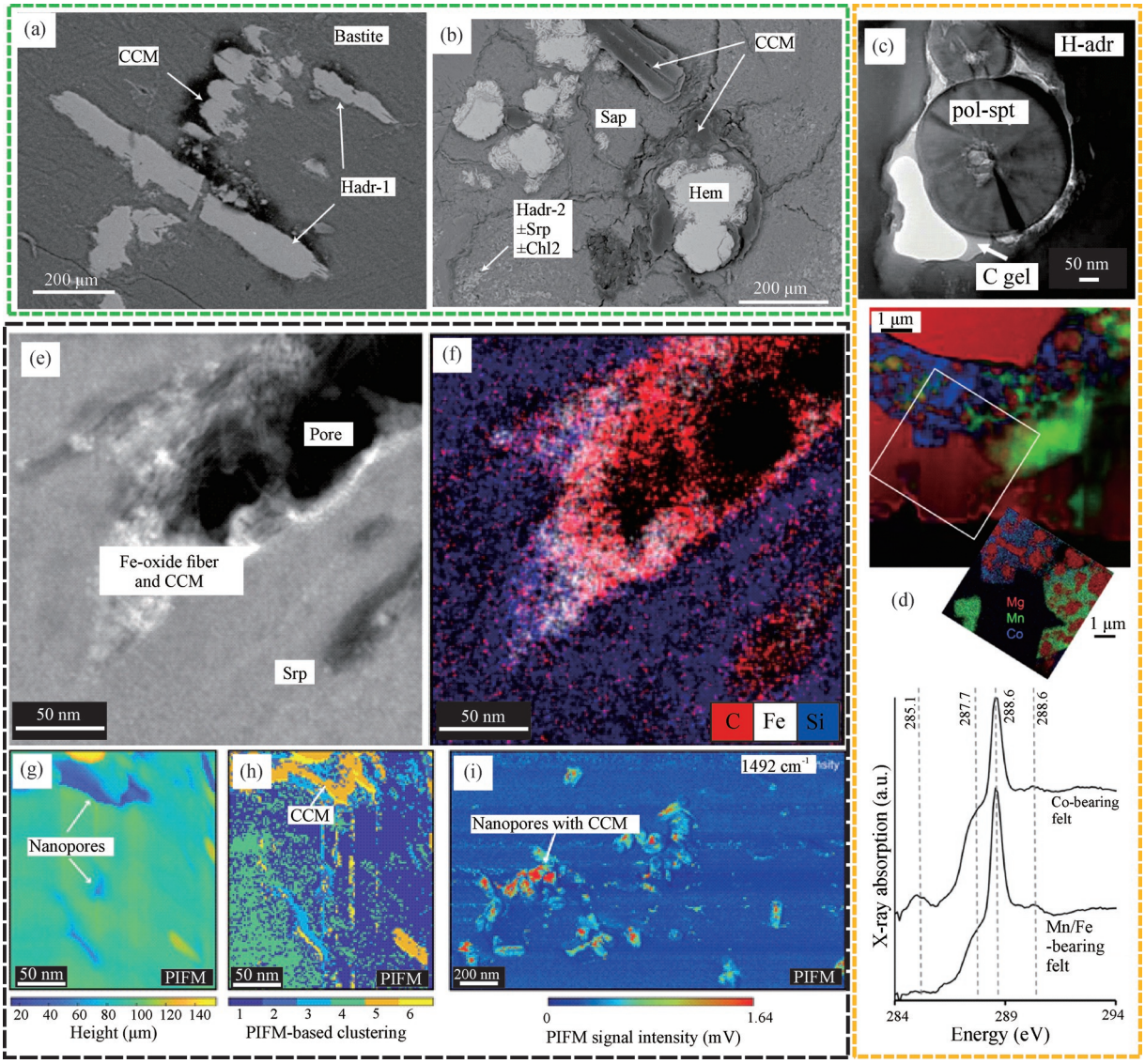

Fig. 4. Solid abiotic organics as the independent condensed carbonaceous matter (CCM) phase in serpentinites.
(a–b) The relationship between minerals and CCM in the Ligurian Tethyan ophiolite (Italy) (from Sforna et al., 2018): (a) association of CCM with hydroandradite and bastite assemblage; (b) large patches of CCM coating hematite and invading microcracks affecting saponite; (c–d) nucleation and growth of polyhedral and polygonal serpentine (pol-spt) from the hydrogarnet (H-adr) dissolution appearing to be mediated by a carbon-bearing gel-like phase (from Ménez et al., 2018a; reprinted with permission from Elsevier, copyright). STXM characterization of the metal-bearing felt enclosed in a fractured hydrogarnet and C-XANES spectra associated with the Co-bearing area and the Mn-enriched felt in (d) showing the presence of aromatic or olefinic carbon (285.1 eV), aliphatic carbon (287.7 eV), carboxyl functional groups (288.6 eV), and carboxyl groups bounded to metals (290.4 eV); (e–i) CCM in serpentinites from the Yap Trench (from Nan et al., 2021); (e–f) spatial association of carbonaceous matter with Fe oxides and serpentinite nanoporosity; (g–i) presence of micron- and nano-sized organic compounds within serpentinite derived by hyperspectral PiFM mapping and aromatic C=C stretching mode at 1492 cm^{-1}.

demonstrating that serpentinization reactions can produce both solid and gaseous/liquid abiotic organic compounds.

Sforna et al. (2018) used scanning electron microscopy (SEM), Raman spectroscopy (Raman), and infrared spectroscopy (FTIR) to elucidate the relationship between minerals and CCM in the Tethyan Ligurian ophiolite, Italy. The strict spatial association between the organic and mineralogical phases suggests that three forms of CCM are in paragenetic equilibrium with secondary mineral phases, during the hydration of mantle-derived ultramafic rocks. With decreasing temperature and increasing oxygen fugacity and SiO_2 activity, the following are observed: (1), hydroandraditic garnets (Hadr) inside bastitized pyroxenes are covered by a carbon film containing aliphatic chains (Fig. 4a); (2), small CCM aggregates (~2 µm) are associated with the alteration rims of spinel and plagioclase pseudocrystals (Hadr ± serpentine ± chlorite); and (3), large CCM aggregates (100–200 µm), bearing aromatic carbon and short aliphatic chains, are associated with a saponite and hematite assemblage after plagioclase (Fig. 4b). Simultaneous precipitation of different CCM species with specific mineral replacement reactions suggests an abiotic endogenic genesis. In addition, Raman and FTIR spectra

lack the features of protein-forming amide groups of biological origin or thermal degradation of pristine biogenic material, which usually display the expected broad bands of graphitic carbon (1340–1360 and 1580–1610 cm^{-1}). Ménez et al. (2018a) used scanning transmission electron microscopy coupled with energy dispersive X-ray spectrometry (STEM-EDXS) and synchrotron radiation-based scanning transmission X-ray microscopy (STXM) coupled with X-ray absorption-near-edge structure (XANES) spectroscopy to characterize the nanoscale structure of a special group of 'andraditic hydrogarnets + polygonal and polyhedral serpentine (pol-spt) + CCM' (Fig. 4c), and demonstrated that abiotic organic compounds are directly involved in low-temperature serpentinization reactions (< 200°C). These compounds are thought to play a role in the formation and stabilization of polyhedral serpentine because of the strict association of the pol-spt serpentine with an Mg- and Si-bearing organic phase, which embeds all spheroid and tubular structures and coats the surface of the hydrogarnets grains. Ménez et al. (2018a) suggested that organic coatings at mineral surfaces might influence the nature and structure of the serpentinization products, as well as the mobility and speciation of transition metals as the reaction progresses. For example, CCMs in the Mn-enriched regions of hydrogarnets display mainly C-XANES absorption features of carboxylic functional groups along with a lower amount of aliphatic carbon and carboxyl groups binding iron; whereas, the Co-enriched regions shown increased and decreased levels in aliphatics and carboxyl functional groups, respectively, plus minor aromatic or olefinic carbon. This provides a paradigm for studying organic-mineral interactions and highlights the affinity of metals with reactive organic functional groups (Fig. 4d). In a similar case, Nan et al. (2021) show the direct association between CCM and a nanosized Fe-oxide phase within serpentinite nanopores (recovered from the Yap Trench, western Pacific Ocean by human-occupied vehicle Jiaolong at 6413 m below sea level; Figs. 4e–f). Vibrational spectroscopy (Photo-induced force microscopy, PiFM) revealed that the CCM contains both aliphatic and aromatic compounds (Figs. 4g–i), but there is no evidence for functional groups typical for biological organics. Abiotic synthesis of both solid and volatile organic compounds by serpentinization may also occur in the shallowest portions of subduction zones. Plümper et al. (2017) observed solid organic matter in serpentinite from mud volcanoes in the Mariana subduction system but speculated that biological processes might be responsible given the low-*T* of formation (<122°C was given as the thermal stability for microbial life). In contrast, Debret et al. (2022) first reported solid organic compounds in higher-*T* serpentinite clasts (~0.5 GPa, 300–400°C) from the Mariana trench and suggested on the basis of correlations between carbon and iron stable-isotope signatures and fluid-mobile element (B, As and Sb) concentrations that the organic compounds are generated through abiotic reduction of CO_2-rich slab-derived fluids, e.g., $2FeCO_3(aq) + 6FeO + 2H_2O(aq) = 4Fe_2O_3 + CH_3COO^- + H^+(aq)$.

Abiotic CCM absorbed onto mineral surfaces is particularly difficult to identify. Ménez et al. (2018b) provides the first evidence that amino acids, the building blocks of biological proteins, can form abiotically at depth during the aqueous alteration of the oceanic lithosphere. These were identified by a combination of high-resolution imaging techniques synchrotron-coupled deep-ultraviolet (S-DUV) and synchrotron-Fourier-transform-infrared (S-FTIR) micro-spectroscopy and time-of-flight secondary ion mass spectrometry (TOF-SIMS). This study found that only Fe-rich saponites contained organic signals of tryptophan, indicating that CCM grew in combination with host minerals but lacked the characteristic functional group signals that biologically formed amino acids would carry, suggesting the amino acids observed were abiotic in origin (Figs. 5a–c). Additionally, TEM analysis showed that the nanopore network of Fe-rich saponite carrying the tryptophan was too small to carry prokaryotic cells, which at minimum are a size of several microns (Figs. 5d–e). To explain these observations, Ménez et al. (2018b) proposed that a Friedel–Crafts-type reaction catalyzed by Fe-rich saponite might have produced the aromatic amino acids during the hydrothermal alteration of peridotite. The potential of fluid-rock interactions to generate amino acids abiotically not only supports the hydrothermal theory for the origin of life but may also shed light on ancient microbial metabolisms and the functioning of the present-day deep biosphere (Ménez, 2020).

In summary, evidence has surfaced over the past 10 years that abiotic geological processes can form small molecules, e.g., CH_4 in hydrothermal vents, to more complex polymeric organics, e.g., aliphatic chains and PAHs (Ménez et al., 2012; Sforna et al., 2018; Nan et al., 2021), and biochemical precursors, e.g., aromatic amino acids (Ménez et al., 2018b). These discoveries may lay the foundations of a deep geological alternative to other theories for the emergence of carbon-based life on other planetary bodies. Furthermore, with increasing depth, rock-hosted solid organic compounds might/could be the main carrier of carbon (Debret et al., 2022), calling for a reappraisal of serpentinized forearc as a major reservoir for abiotic production and storage of organic carbon in subduction systems. Because of the small size (down to the nanoscale) and/or high C:H ratio of CCMs (like IOM in carbonaceous chondrites), in situ high-resolution imaging and compositional analytical instrumentation provides the improved characterization of abiotic solid organic compounds, namely: (1) imaging of textural relationships between CCM and associated minerals, and (2) providing the ability to identify the presence or absence of compositional biomarkers. To date, such studies have focused on crustal-level serpentinite, but represent a promising avenue of investigation for abiotic solid organic compounds in the deep subduction zone and mantle rocks.

4.1.2 Perspectives from thermodynamics and experimental simulations

Serpentinization, which produces H_2, drives F–T-type reactions (CO_2 hydrogenation) in a hydrothermal environment (e.g., $CO_2 + 4H_2 \leftrightarrow CH_4 + 2H_2O$, $CO_3^{2-} + 4H_2 \leftrightarrow CH_4 + H_2O + 2OH^-$). LT and HP conditions are thermodynamically favorable for CO_2 methanation

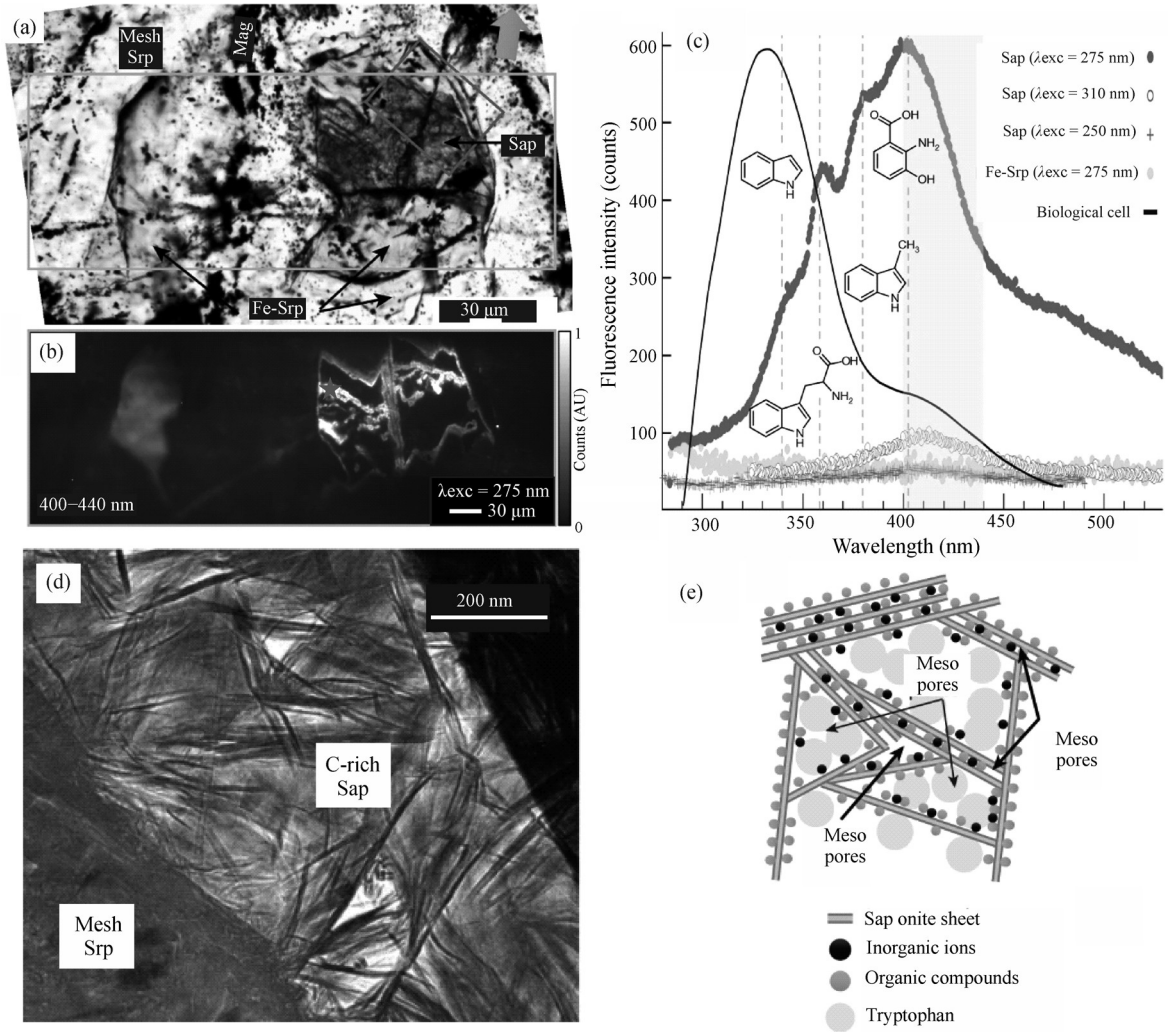

Fig. 5. Abiotic organics absorbed inside Fe-rich soapstone in marine serpentinites (from Ménez et al., 2018b; reprinted by permission from Springer Nature, copyright).

(a–c) Endogenous UV-autofluorescence locally revealed by S-DUV imaging: (a) optical image; (b) full-field S-DUV image of the area depicted by the light-green rectangle in (a) collected between 400 and 440 nm using excitation (λexc) at 275 nm; (c) fluorescence emission spectra collected with excitation wavelengths of 250, 275 and 310 nm, respectively, at the location shown by an asterisk in (b). The spectrum of Fe-rich saponite displays fluorescence characteristics of indole at 340 nm, tryptophan at 358 nm, skatole at 380 nm, and hydroxyanthranilic acid at 403 nm. Fluorescence emission spectra collected at 275 nm in the Fe-rich serpentine and the typical emission spectrum of a biological cell mainly arising from protein-forming tryptophan are shown for reference to demonstrate the absence of biomarker signatures in CCM; (d–e) saponite shows the presence of aggregates formed by the packing of sheets opening nanopores, and suggests the occurrence of pillaring processes and high reactivity of the clay. Packing in the face-face, edge-edge, or edge-face mode results in a house-of-card structure that acts as microreactors for the formation of tryptophan at the acid sites of the Fe-rich saponite.

because F–T reactions are reversible and highly exothermic (Le et al., 2017). Interestingly, Milesi et al. (2016) calculated the $\log\alpha H_2 - \log\alpha CO_2$ phase diagram in the Fe–Mg–C–H–O system from 150°C to 450°C under the pressure condition of 35 MPa and found that besides fluid hydrocarbon components such as the $HCOOH_{(aq)}$, $CH_3COOH_{(aq)}$, the solid carbonaceous matter would precipitate below 400°C in a disordered, amorphous form, e.g., hydrogenated carbonaceous materials, rather than as crystalline graphite.

Berndt et al. (1996) were the first experimentally conduct serpentinization reactions, which included the reaction of fayalite with aqueous sodium bicarbonate at 300°C and 50 MPa. As serpentinization progressed, they observed that concentrations of several light hydrocarbons (CH_4, C_2H_6, and C_3H_8) and H_2 increased during the experiment, whereas the concentration of total dissolved CO_2 (CO_2 (aq) and HCO_3^-) decreased; reaction products were found to contain magnetite, serpentine, and aromatic solid carbon with aliphatic chains. Later, McCollom et al. (1999), McCollom and Seewald (2006), McCollom (2016), and Seewald et al. (2006) carried out a large number of similar experiments at 17–35 MPa and 150–350° C, such as $NaHCO_3$/NaHCOO/CO/HCOOH ± fayalite/Fe^0 ± H_2, and traced the experimental products by ^{13}C labeling. These experiments demonstrate that increasing the concentration of H_2 is beneficial to the production of CH_4, but, without a catalyst, these F–T-type reactions produce CH_4 at a slow rate; the reaction time varies from several thousand to ten thousand hours. In

Table 1 Experiments results of hydrogenation of carbonates

Reactants	Pressure (bar)	Temperature (℃)	Inorganic products	Methane production (mol%)	Other organic gases	Reference
$CaCO_3 + H_2$	137–275	535–735	CaO, $Ca(OH)_2$, H_2O, CO, C^0	0.05–2.67	C_2H_6	Giardini et al., 1968
$CaMg(CO_3)_2 + H_2$	137–344	520–835	$CaCO_3$, $Ca(OH)_2$, CaO, $Mg(OH)_2$, H_2O, CO, CO_2, C^0	0.01–4.76	C_2H_6	Giardini et al., 1969; Reller et al., 1987
$FeCO_3 + H_2$	137–344	400–605	Fe, FeO, Fe_3O_4, H_2O, C^0	0.15–4.45	C_2–C_4	

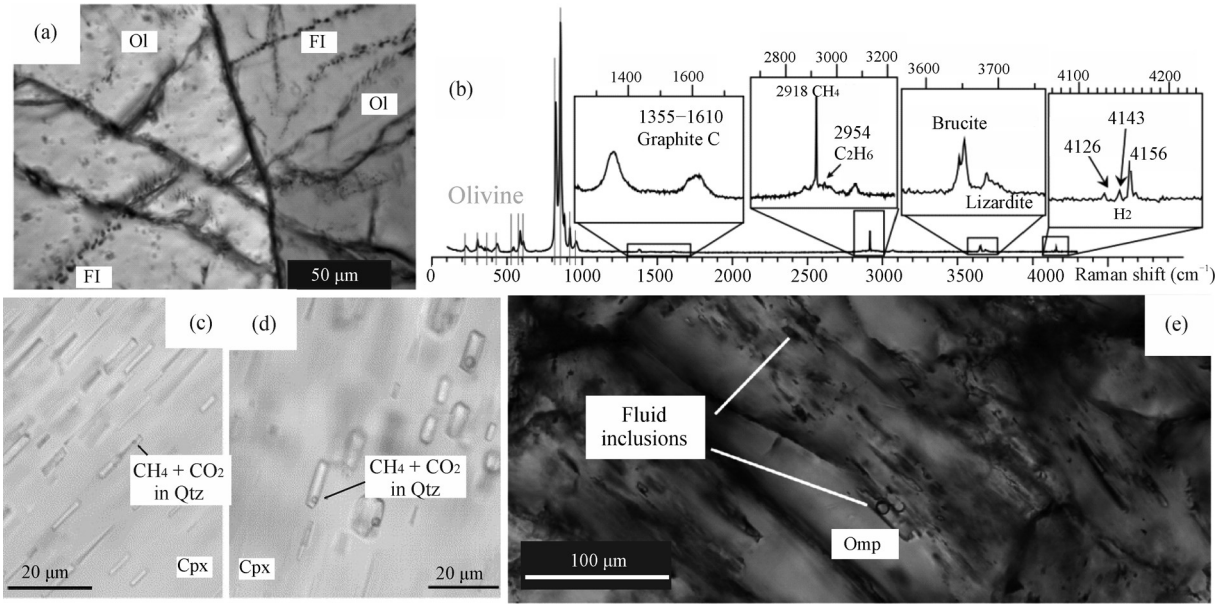

Fig. 6. Abiotic light hydrocarbons in natural (U)HP metamorphic rocks from subduction zones.
(a–b) CH_4-C_2H_6 fluid inclusions and their Raman spectra in olivine in partially serpentinized peridotite from the Italian Alpine subduction zone (modified after Brovarone et al., 2020); (c) CH_4-CO_2 fluid inclusions in Na-rich clinopyroxene in coesite-bearing continental-type eclogites in the Dabie–Sulu metamorphic belt (modified after Fu et al., 2003 and reprinted with permission from Elsevier, copyright); (d) CH_4 fluid inclusions in omphacite in carbonated oceanic-type HP eclogites in the southwestern Tianshan subduction zone (from Tao et al., 2018).

contrast, the reduction of dissolved CO_2/HCO_3^- to HCOOH, CO, CH_3OH under hydrothermal conditions can occur within a few days, even at temperatures as low as 175°C, suggesting that a very long geological timespan or the presence of catalysts is critical.

In addition to CO_2 hydrogenation, the hydrogenation of carbonates is also an effective way to produce hydrocarbons (Table 1). Giardini et al. (1968) proposed that calcite could react with hydrogen ($CaCO_3 + H_2$) to form CaO, $Ca(OH)_2$, H_2O, CO, CH_4, C_2H_6, and C^0 at pressures of 600–800 bar and temperatures of 500–850°C. Shortly after, Giardini and Salotti (1969) carried out a hydrogenation reaction for dolomite and siderite. Such reactions can be summarized as $MCO_3 + H_2 \rightarrow C^0 + HCs + H_2O + MO$ or $M(OH)_2$ and reach equilibrium within a few hours (Reller et al., 1987) and may be possible in subduction zones where carbonate and serpentinite are subducted to deep metamorphic conditions.

4.2 High-pressure subduction zone system (crust-mantle interaction level)

4.2.1 Petrological investigations

Hydrocarbon-bearing fluid inclusions, e.g., CH_4, have been recognized in minerals from exhumed high to ultrahigh-pressure (HP–UHP) terranes and as inclusions in subduction-related diamonds from kimberlite pipes. For example, Frezzotti (2019) found that micro-diamonds in fluid inclusions from metamorphic sediments from Lago di Cignana, Italy, are coated with carboxylic acids ($COOH^-$), indicating the synthesis of complex organic compounds in deep fluids. Brovarone et al. (2017, 2020), Boutier et al. (2021), and Peng et al. (2021) observed CH_4 ($\pm H_2 \pm C_2H_6 \pm H_2S \pm NH_3$)-rich fluid inclusions in HP-LT metamorphosed ultramafic rocks (Figs. 6a–b) from the western Italian Alps, Appalachian belt, and S.W. Tianshan, respectively, which demonstrates that deep serpentinization (40–80 km) in subduction zones might generate reduced C–O–H(–N–S) fluids.

To date, most observations of deep abiotic organic molecules are associated with subducted ultramafic rocks; however, the presence of these molecules in subducted mafic crust remains more enigmatic. For example, Fu et al. (2003) and Mukherjee and Sachan (2009) discovered CH_4-bearing fluid inclusions in quartz in UHP continental eclogites (Figs. 6c–d) in the Dabie–Sulu and Himalayan metamorphic belts; however, it was not clear how these fluids originated. Recently, Tao et al. (2018), Wang et al. (2022), and Zhang et al. (2023) reported CH_4-rich fluid inclusions from oceanic-type mafic eclogite from the HP-UHP S.W. Tianshan metamorphic belt (Fig. 6e). Based on garnet (Grt)–clinopyroxene (Cpx) oxybarometry, the fO_2 was sufficiently low (FMQ−3) such that the graphite-

saturated C–H–O fluid contained CH_4 as the dominant volatile carbon species (Wang et al., 2022). To date, CH_4 appears to be the most common hydrocarbon species hosted in HP-UHP rocks. However, all or some of the CH_4 present in these inclusions might form through the decomposition or degradation of more complex organic-bearing fluids. Indeed, the presence of daughter minerals, such as graphite, calcite, etc., clearly indicates that some carbon redistribution occurs within the fluid inclusions (Sverjensky, 2020).

4.2.2 Thermodynamic constraints

Sverjensky et al. (2014) used the DEW model to calculate the aqueous C-speciation in equilibrium with a metasedimentary eclogite under the conditions of 600–1000°C, 5 GPa, and log fO_2 = FMQ−2, predicting that significant aliphatic organic species, such as propionate and formate, are coexistent with CO_2 and CH_4. Particularly, the reduced abiotic organic species, e.g., $HCOO^-$, CH_4, are predicted to be more abundant than oxidized carbon species, e.g., CO_2, HCO_3^-, at HP-LT conditions (Fig. 7a). Connolly and Galvez (2018) coupled the DEW thermodynamic database with the Holland and Powell (2011) database in Perple_X (Connolly, 2005), allowing for the simultaneous modeling of both solute species and complex solid solution phases as a function of *P*-*T*-X; they predicted that fluids released from average subducted sediments will stabilize formate at pressures above 3 GPa (Fig. 7b).

The same approach developed by Connolly and Galvez (2018) has been applied to simulate dissolved carbon species released during the metamorphism of real rocks. For example, Wang et al. (2022) used this method to investigate the factors stabilizing CH_4 during metamorphism of UHP mafic eclogite. In coesite-bearing eclogites, garnet cores and mantles and omphacite cores have been observed to contain primary $CH_4 + H_2O$ (± H_2) fluid inclusions, as well as core TFeO and $Fe^{3+}/\Sigma Fe$ ratios that were elevated relative to garnet and omphacite rims (Figs. 8a–b). Thermodynamic phase equilibrium calculations for the *P*–*T* path and garnet-clinopyroxene oxybarometry together reveal that UHP-CH_4 eclogites can reach an fO_2 condition of about FMQ−3 at their peak *P*-*T* conditions (2.8 GPa, 525°C), consistent with the formation of CH_4 under rock buffered conditions (i.e., $8(Fe^{2+}O)_{mineral} + CO_2 + 2H_2O \leftrightarrow 4(Fe^{3+}{}_2O_3)_{mineral} + CH_4$). In contrast, the early exhumation stage of metamorphism (2.5 GPa, 600°C) resulted in higher fO_2 conditions of FMQ−0.8. Thermodynamic models show that this change in fO_2 is primarily driven by the slight change in temperature between peak and early retrograde conditions, where low fO_2 is predicted at lower *T*, whereas fO_2 is less sensitive to the pressure drop, with lower fO_2 predicted at higher *P* at fixed *T*. Furthermore, a comparison was made with an HP eclogite from the same terrane in which CO_2-rich inclusions were observed; Wang et al. (2022) found that the higher bulk CO_2 content and elevated $Fe^{3+}/\Sigma Fe$ ratio inherited from pre-subduction alteration, prohibited sufficiently low fO_2 to produce CH_4. However, fO_2 conditions between FMQ and FMQ+1 were low enough to stabilize graphite via auto-redox adjustments (O_2 + $(Fe^{2+}O)_{mineral} \leftrightarrow (Fe^{3+}{}_2O_3)_{mineral}$, $O_2 + C^0 \leftrightarrow CO_2$) at 2.6 GPa, 500°C. Therefore, a combination of lower-*P* and higher-*T* with an elevated redox budget (RB), controlled by the amount and oxidation state of all redox-sensitive major elements, e.g., Fe, C, and S (Evans 2006), stabilized CO_2 over CH_4 under rock-buffered conditions. Importantly, the loss of oxidized or reduced species from a rock will change the RB of the remaining rock. For

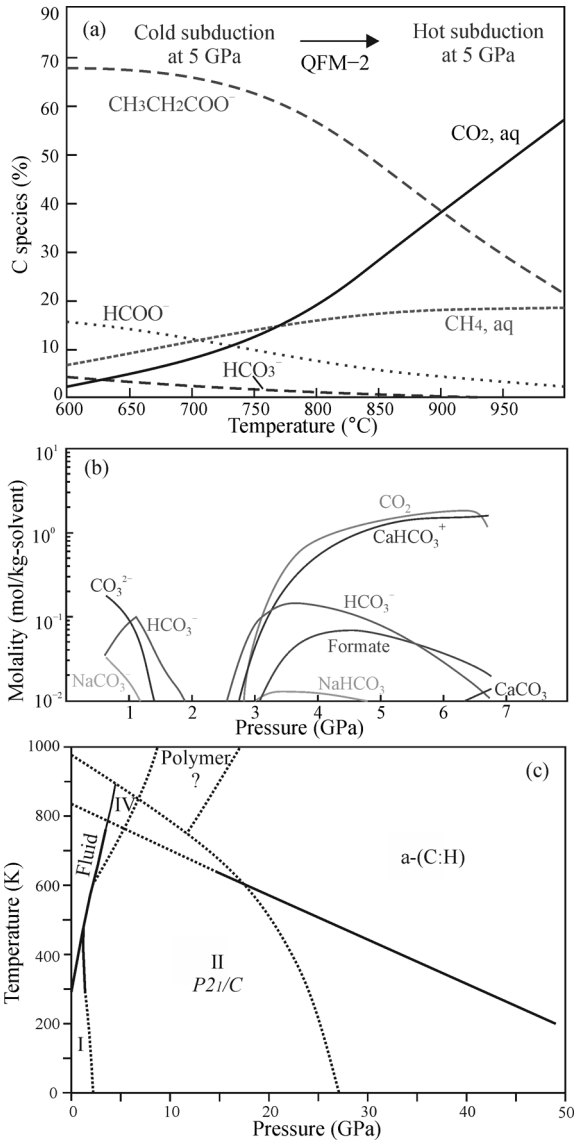

Fig. 7. C–H species in subduction zones constrained by thermodynamic models.

(a) Aqueous C-speciation in equilibrium with a model metasedimentary eclogite containing diamond, jadeite, pyrope, kyanite and coesite at 5.0 GPa and a range of temperatures from cold to hot subduction zones (modified after Sverjensky et al., 2014; reprinted by permission from Springer Nature, copyright). Ionic organic carbon species such as propionate are predicted to be abundant in the cold subduction-zone fluids; (b) carbon-fluid speciation in closed-system devolatilization of the GLOSS sediment composition using the lagged speciation calculation algorithm (modified after Connolly and Galvez, 2018; reprinted with permission from Elsevier, copyright) along the subduction zone geotherm; (c) phase diagram and chemical-stability boundary of benzene (modified after Ciabini et al., 2007; reprinted by permission from Springer Nature, copyright).

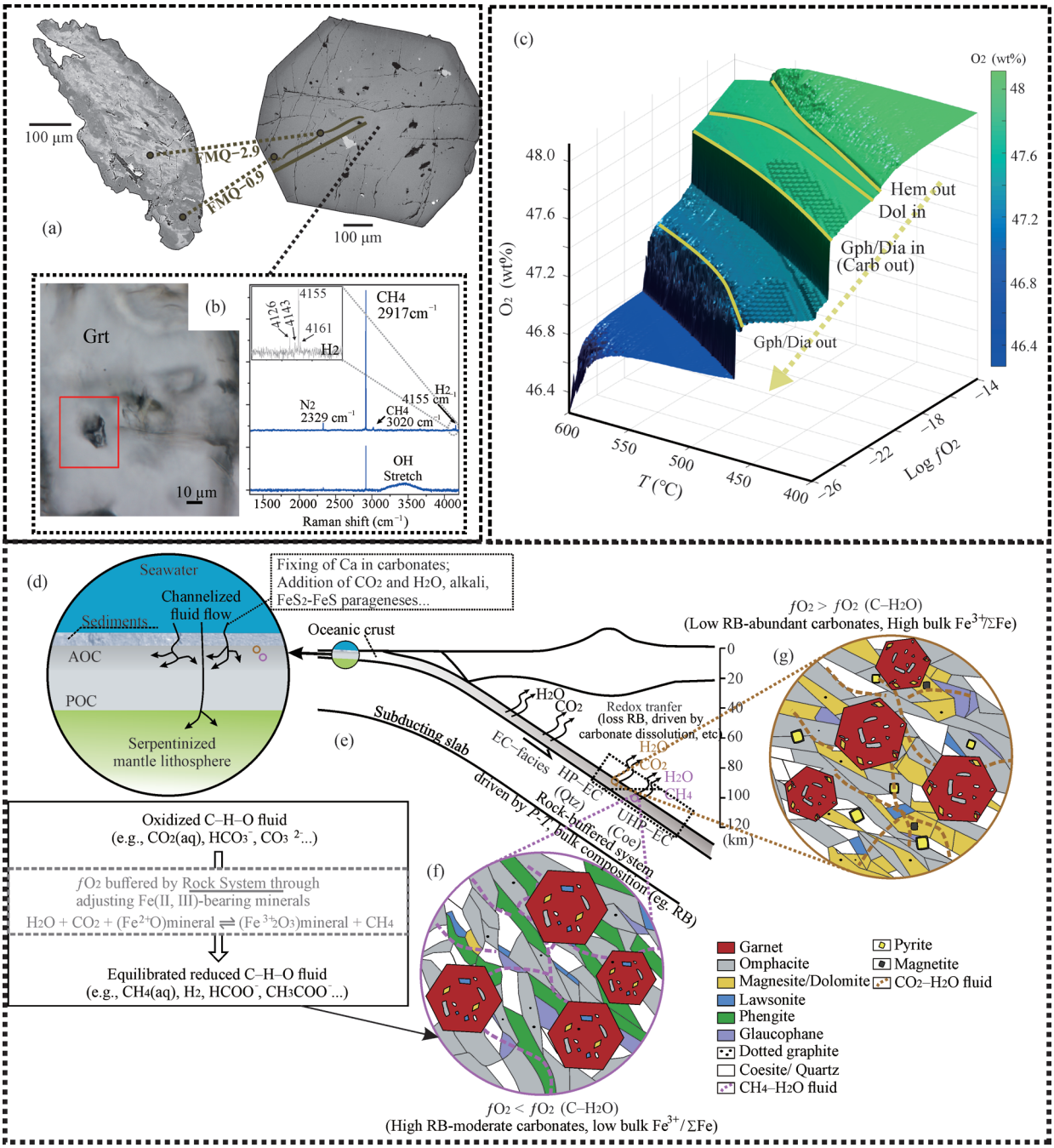

Fig. 8. Formation of abiotic CH_4 in subducted oceanic crusts (modified after Wang et al., 2022; reprinted with permission from Elsevier, copyright).

(a–b) CH_4-bearing garnet and omphacite in the coesite-bearing (UHP-CH_4) eclogite that clearly shows two sets of garnet–omphacite pairs (omphacite cores–garnet cores, omphacite rims–garnet rims), which were used to constrain the fO_2 condition using Grt–Cpx oxybarometry; (c) three-dimensional O_2–T–log fO_2 diagram for the UHP-CH_4 eclogite, which was modeled using changes in excess O_2 emphasizing the impact of the redox budget on rock oxygen fugacity and mineral stability. (d–g) Schematic view of the condition of P–T–X–fO_2 for a mafic oceanic slab during subduction (e.g., palaeo S.W. Tianshan subduction zone). (d) Bulk-composition modification of oceanic slabs prior to subduction during heterogeneous hydrothermal alteration, leading to different initial redox budgets. The pink and brown circles represent the possible positions of CH_4- and CO_2- rich eclogites in the lithosphere before subduction respectively; (e) The release of oxidized or reduced slab fluids depends on both the P-T conditions and the composition of the slab in the rock-buffered system. Depending on the degree to which the redox budget decreases, prograde redox reactions may stabilize different carbon species in the C–H–O fluid at variable depth levels during subduction; (f) The eclogite, combined with moderate bulk CO_2 content and low Fe^{3+}/SFe, stabilizes CH_4-rich fluids at their metamorphic peak; (g) The eclogite, combined with higher bulk CO_2 content and elevated Fe^{3+}/SFe, stabilizes CO_2-rich fluids at their metamorphic peak.

example, CH_4-bearing fluids were lost during prograde to peak metamorphism whereas Fe^{3+} remained, and, as a result, the remaining rock is more oxidized once a new equilibrium is reached, which might have contributed to the higher fO_2 recorded by garnet and omphacite rims. This scenario highlights the need to consider both redox

couples and open system behavior when interpreting fO_2 and corresponding C aqueous species. Small changes in the RB of a rock during open system processes may lead to large changes in fO_2, particularly when a buffering assemblage is consumed or changed (Fig. 8c). As a consequence, the thermal structure (*P-T* conditions) of the subduction zone and the composition of the slab, in response to the protolith alteration before subduction and changes to the total RB as mobile elements are extracted during subduction, are first-order controls on the redox evolution of the subducting slab and carbon speciation in slab fluids (Figs. 8d–g). Among them, the cold subduction of a weakly altered oceanic crust may provide ideal conditions for the formation of ultra-deep abiotic CH_4.

4.2.3 High-pressure experimental constraints

Some major experimental insights and comments (summarized in Table 2) are subdivided into the following specific approaches:

(1) Hydrogenation of graphite/diamond

Sharma et al. (2009) heated graphite above 1500°C in an H_2 atmosphere at 5–6 GPa and found that CH_4, C_2H_6, and unsaturated aromatic hydrocarbons were produced. Similarly, Peña-Alvarez et al. (2021) conducted diamond/graphite hydrogenation experiments under subduction-zone *P-T* conditions (1–4 GPa, 330–730°C) in which CH_4 formed directly from the reaction of elemental carbon (diamond, graphite, or amorphous carbon) with hydrogen. Additionally, C_2H_6 was also produced at the highest experimental temperature (730°C).

(2) Water-driven reduction reactions of carbonates at low oxygen fugacity conditions

Kutcherov et al. (2002) used $CaCO_3 + H_2O + FeO$ as starting materials to synthesize saturated hydrocarbons up to undecane at 3–5 GPa and 1200°C, with associated magnetite (Fe_3O_4) and calcium hydroxide ($Ca(OH)_2$) reaction products. Scott et al. (2004) similarly used $CaCO_3 + H_2O + FeO$ as reactants, observing the formation of CH_4, Fe_2O_3–Fe_3O_4, and calcium ferrite ($CaFe_5O_7$, $CaFe_4O_7$ or $CaFe_2O_4$) in the DAC sample chamber over the *P-T* range 5–11 GPa and 600–1500°C; immiscible of CH_4 bubbles and water can form during decompression and cooling. However, Sharma et al. (2009) did not detect any CH_4 by Raman spectroscopy in an experiment with $CaCO_3 + H_2O + FeO$ at 4 GPa and 350°C, suggesting higher temperatures are required to produce CH_4. Mukhina et al. (2017) carried out experiments in the $CaCO_3 + H_2O$ system with Fe^0 over the *P-T* range 2.0–6.5 GPa and 250–600°C, finding that the formation of hydrocarbons is strongly controlled by temperature compared to pressure, as CH_4 can be produced as long as the temperature is higher than 250°C over the experimental pressure range. Additionally, they found that the abundance of CH_4 increases with increasing temperature. Although CH_4 was the main component (95 vol%) in the system, alkanes up to heptane, as well as unsaturated aromatics–benzene, were also detected. Chen et al. (2008) conducted experiments at 550°C, 5.0–6.5 GPa in the following chemical systems: (1) $CaCO_3 + FeO + H_2O$; (2) $CaCO_3 +$ FeO + serpentine; (3) $CaCO_3 +$ fayalite + H_2O; (4) $CaCO_3 + SiO + H_2O$. All experiments were found to produce CH_4 accompanied by CO_3^{2-}. Graphite (C^0) was not reported in the products. If a strong reducing agent, such as Fe, FeO, or SiO, is included, the general formula of the reaction between $CaCO_3$ and H_2O to produce CH_4 is $CaCO_3 + H_2O$ (in fluid or mineral) + Fe^{2+} or Fe^0 (in mineral) → Ca^{2+} (in mineral and fluid) + CO_3^{2-} + Fe^{2+} − Fe^{3+} (in mineral) + HCs. It is worth noting that the experimental studies cited here focus on the reduction reaction of $CaCO_3$, which is geologically meaningful as $CaCO_3$ is the most abundant carbonate in the seafloor. However, $CaCO_3$ will gradually react with silicate phases and significant solid solution with or separate phases of $MgCO_3$ may form to the lower mantle conditions. Therefore, it may be important for future experiments to examine the effects that a $MgCO_3$ component or mineral can play in the deep mantle at reducing conditions with saturated Fe–Ni metal alloys.

(3) Water-driven disproportionation reactions with carbonates

Thermal decomposition of $FeCO_3$ (siderite) is observed between 350°C and 400°C at 1 bar with magnetite and scarce graphite formed as reaction products. Such experiments indicate the potential for disproportionation of carbon to different valence states (Wang et al., 2023). In an H_2O-rich environment, some fascinating chemical reactions are generated. Weng et al. (1999) reacted siderite with water to produce CH_4 and C_2H_6 at 1 GPa and 800–1500°C using a laser-heated DAC (LH-DAC) combined with gas chromatography analysis technology. This study suggests the following abiotic CH_4 production mechanism: $FeCO_3 + H_2O \rightarrow CH_4 + CO + O_2 + Fe_3O_4$. McCollom (2003) conducted similar experiments at 300°C and ≤100 bar and proposed instead the reaction: $FeCO_3 + H_2O \rightarrow H_2 + CO + CO_2 + Fe_3O_4 +$ HCs. In addition to C_1–C_4 light hydrocarbons, abundant aromatic compounds containing alkyl and hydroxyl groups were synthesized. In the next advancement, Marocchi et al. (2011) monitored the reaction process of $FeCO_3$ and H_2O at ~1 GPa and 250 to 400°C using in situ Raman spectroscopy. They found that: (1) at 250°C formaldehyde (HCOH) was formed near the surface of siderite, (2) at >250°C formic acid (HCOOH) and carbon monoxide (CO) were detected with graphite and magnetite, and (3) formaldehyde can be formed at a lower temperature of 130°C when siderite reacts in the presence of an aqueous solution containing NaCl, enhancing the dissolution of siderite and the formation of organic chloride molecules. However, CH_4 was not synthesized in all of their experiments. In a similar study, Tao et al. (2018) reacted Fe-rich dolomite ($Ca_{1.02}(Fe_{0.52}Mg_{0.43}Mn_{0.04})(CO_3)_2$)) with H_2O at 1.5–6 GPa and 800–1200°C to produce C_1–C_4 light hydrocarbons and graphite.

To summarize, the disproportionation of Fe-bearing carbonates with water at high temperatures takes the following form: Fe^{2+} (in mineral) + C^{4+} (in mineral) + $H_2O \rightarrow Fe^{3+}$ (in mineral) + C^0 + HCs. However, the products of this reaction as a function of P–T are inconsistent between studies. First, Marocchi et al. (2011) synthesized formaldehyde and formic acid under medium pressure and high temperature conditions but did not detect CH_4, instead proposing that CH_4 formation has kinetic obstacles that were not overcome in the experiments. In contrast,

Table 2 Summarized experimental results related to the high-pressure subduction zone system

Type of reaction	General reaction formula	Reactants	Pressure (GPa)	Temperature (°C)	Products of organics	Products of solids	Reference	Comments to results
Hydrogenation of elemental carbon	$C + H_2 \rightarrow CxHy$	Diamond/graphite/amorphous carbon + H_2	1–4	330–730	$CH_4 + (C_2H_6)$	Not report	Peña-Alvarez et al., 2021	Heavier hydrocarbons can be produced at higher temperatures.
			5–6	>1500	C_1–C_2 + Aromatics/Olefins	Not report	Sharma et al., 2009	
Water-driven disproportionation reactions with carbonates	Fe^{2+} (in mineral) + C^{4+} (in mineral) + $H_2O \rightarrow Fe^{3+}$ (in mineral) + C^0 + HCs	Siderite + H_2O	<100 bar	300	C_1–C_4+Aromatic compounds containing alkyl and hydroxyl groups	Fe_3O_4	McCollom, 2003	
			0.7	400	HCOOH, HCHO	C^0; FeO; Fe_3O_4; Fe_2O_3	Marocchi et al., 2011	No CH_4?
		Fe-Dolomite+ H_2O	1.6–6	800–1200	$C_1 + (C_2$–$C_4)$	C^0; Fe_3O_4	Tao et al., 2018	
Water-driven reduction reactions of carbonates at low fO_2 conditions	$CaCO_3 + H_2O$ (in fluid or mineral) + Fe^{2+} or Fe (in mineral) → Ca^{2+} (in mineral and fluid) + Fe^{2+}-Fe^{3+} (in mineral) + HCs + CO_3^{2-}	Calcite + FeO + H_2O	3–5	1200	C_1–C_{11}	Fe_3O_4; $Ca(OH)_2$	Kutcherov et al., 2002	Unreasonable to press $CaCO_3$ all the way down to more than 10 GPa. At depths ≤ 250 km, the redox conditions for FeO-Fe metal saturation are almost impossible.
			6.5	620	CH_4	Fe_3O_4; Fe-Ca carbonates	Sharma et al., 2009	
			5–6.5	550	CH_4	Not report	Chen et al., 2008	No C^0?
			5–11	600–1500	CH_4	Fe_3O_4; Calcium ferrite($CaFe_5O_7$, $CaFe_4O_7$,$CaFe_2O_4$)	Scott et al., 2004	
		Calcite + Fe-FeO + H_2O	6–7	520–550	CH_4	Fe(CO)x; Fe-Ca carbonates	Sharma et al., 2009	
		Calcite + FeO + Serpentine	5–6.5	550	CH_4	Not report	Chen et al., 2008	
		Calcite + Fayalite + H_2O						
		Calcite + Fe + H_2O	2–6.5	300–600	C_1–C_7 + Unsaturated hydrocarbons-benzene	FexO	Mukhina et al., 2017	

McCollom (2003) synthesized CH_4 and aromatic hydrocarbons at LP-HT conditions and Tao et al. (2018) synthesized CH_4 and other light hydrocarbons at extreme high *P-T* conditions. Such differences may reflect different *P-T-f*O_2 conditions or experimental issues, such as disequilibrium. Systematic research over different *P-T-f*O_2 conditions is required to identify the cause of the discrepancies between studies with regards to CH_4 stability. In addition to Fe, other multivalent metals in carbonates, particularly Mn, may produce similar redox reactions, which have not been constrained experimentally yet.

(4) Polycondensation reactions in an H_2O-free system

In addition to CH_4, the stability of other hydrocarbons at high pressure has been explored. For example, a study on *n*-hexane (C_6H_{14}) conversion using DAC-coupled CO_2 laser heating showed that at 5 GPa and 1200 K, *n*-hexane disproportionated into C^0 and CH_4 (Lobanov et al., 2013). Additionally, C=C and C≡C bonds were detected by Raman spectroscopy at 40 GPa and 2000 K. Further, Yang et al. (2021) synthesized hydrogenated graphitic carbon instead of pure graphite by heating n-hexane at 1000 K and 8 GPa, which is an intermediate product between alkane and graphite that is caused by incomplete dehydrogenation pyrolysis. They proposed that in the range of 2–20 GPa, the pyrolysis temperature of n-hexane and cyclohexane is much lower than that of CH_4. In addition to these studies on long-chain alkanes, this conclusion seems to be suitable for other studies on the stability of unsaturated hydrocarbons. The polymerization of ethylene (C_2H_4) proceeds spontaneously, to form polyethylene, at room temperature above 3 GPa, but the reaction time exceeds 1 month (Chelazzi et al., 2004). Propylene (C_3H_6) can be polymerized at temperatures below 473 K at 1.0 GPa. Increasing the pressure favors polymerization at lower temperatures such that at 3.5 GPa polymerization begins at 300 K (Citroni et al., 2005). Acetylene (C_2H_2) is a solid at room temperature at 0.7 GPa and polymerization occurs at 3.5 GPa, and a transition can be completed in 13 hours (Aoki et al., 1989). Block et al. (1970) observed in an in situ DAC experiment that benzene (C_6H_6) first decomposes into a reddish-orange liquid and finally into amorphous hydrocarbons during heating from room temperature to 880 K gradually at ~4 GPa. Ciabini et al. (2007) combined DAC experiments with first-principles molecular-dynamics calculations to determine the high-pressure phase diagram of benzene (Fig. 7c): the pressure threshold for benzene stability was found to decrease with increasing temperature, with graphite, benzene polymers, and an unknown C–H as the high-*T* products of benzene. PAHs include naphthalene, anthracene, pentacene, perylene, and coronene; Chanyshev et al. (2015) used large-volume press (LVP) assembles to heat PAHs at 7–8 GPa from 773 to 973 K and found oligomeric products up to 3400 Da (Da: Dalton, 1 g/mol) after heating to 773 K and nanocrystalline graphite after heating to 883 K.

(5) Polycondensation reactions in aqueous solutions

The stability and speciation of organic compounds in aqueous systems have been of increasing interest in recent years. Huang et al. (2017) used DAC to explore the high-pressure stability of an aqueous sodium acetate solution (CH_3COONa, 1.0 molal) at 300° C and ~3.0 GPa, showing that aqueous sodium acetate can react to form immiscible hydrocarbons, mainly isobutane, some CH_4, and oxidized carbon-species such as CO_3^{2-}, HCO_3^- and Na_2CO_3 crystals (Figs. 9a–b). Further, Szlachta et al. (2022) conducted similar experiments at higher temperatures and pressures (up to 5 GPa, 600°C) (Fig. 9c), finding that partial decomposition of aqueous sodium acetate to propane, isobutane, and graphitic carbon occurs over the *P-T* range 2–3 GPa and 150–400°C. Additionally, from 4.0 GPa and 500°C to 5 GPa and 600°C, acetate was no longer detected in either in situ hot or quenched liquid by Raman spectroscopy, instead highly disordered kerogen-like carbonaceous materials were found. Similarly, Li (2017) explored the stability of an aqueous formic acid (HCOOH) solution containing NaCl buffered over an *f*O_2 range of Fe–FeO to Re–ReO_2 at 600°C and 700°C from 0.2 to 2.5 GPa. This study demonstrated that CH_4 is produced at *f*O_2 conditions corresponding to the Ni–NiO, Fe–FeO, and Co–CoO buffers. The synthetic fluid inclusions showed evidence of trapping two immiscible fluids, one aqueous and one CH_4-rich, and under the most reducing conditions, i.e., with the Fe–FeO buffer, C_2H_6, H_2, and aromatic rings were detected in CH_4-rich fluid inclusions (Li, 2017; Fig. 9d).

5 Limitations and Challenges

At present the main pathways for synthesizing abiotic organic compounds on earth are: (1) extraterrestrial origin, such that macromolecular organics formed by stellar processes are inherited and preserved in the early Earth; (2) F–T-type (carbon dioxide hydrogenation in a broad sense) reactions in hydrothermal environment where hydrogen is derived from serpentinization of ultramafic rocks or by radiolysis of water; (3) CH_4–H_2-dominated C–H–O fluid formed at low oxygen fugacity (e.g., Fe^0-saturation) conditions in the deep mantle; (4) thermodynamic re-equilibration of C–H–O during magma cooling, degassing, and alteration; (5) hydrogenation of graphite/diamond; (6) hydrogenation of carbonate; (7) water-driven reduction reactions of carbonates at low *f*O_2 conditions, e.g., in the presence of Fe/FeO; (8) water-driven disproportionation reactions with carbonates, e.g., siderite, Fe-bearing dolomite; (9) polycondensation reactions after synthesis of low-molecular-weight organic compounds; and (10) hydration reactions in aqueous solutions after synthesis of low-molecular-weight organic compounds.

Overall, these reactions are found to be sensitive to *P*, *T*, and *f*O_2. Following abiotic synthesis of these organic molecules (generally light hydrocarbons), organic-organic phase transitions or organic-mineral interactions can occur to generate heavy hydrocarbons in different geological environments, e.g., subduction progress, or heating by mantle plumes. Therefore, the classification of abiotic organic compounds on Earth should include inorganic → organic, organic ↔ organic, and organic ↔ mineral

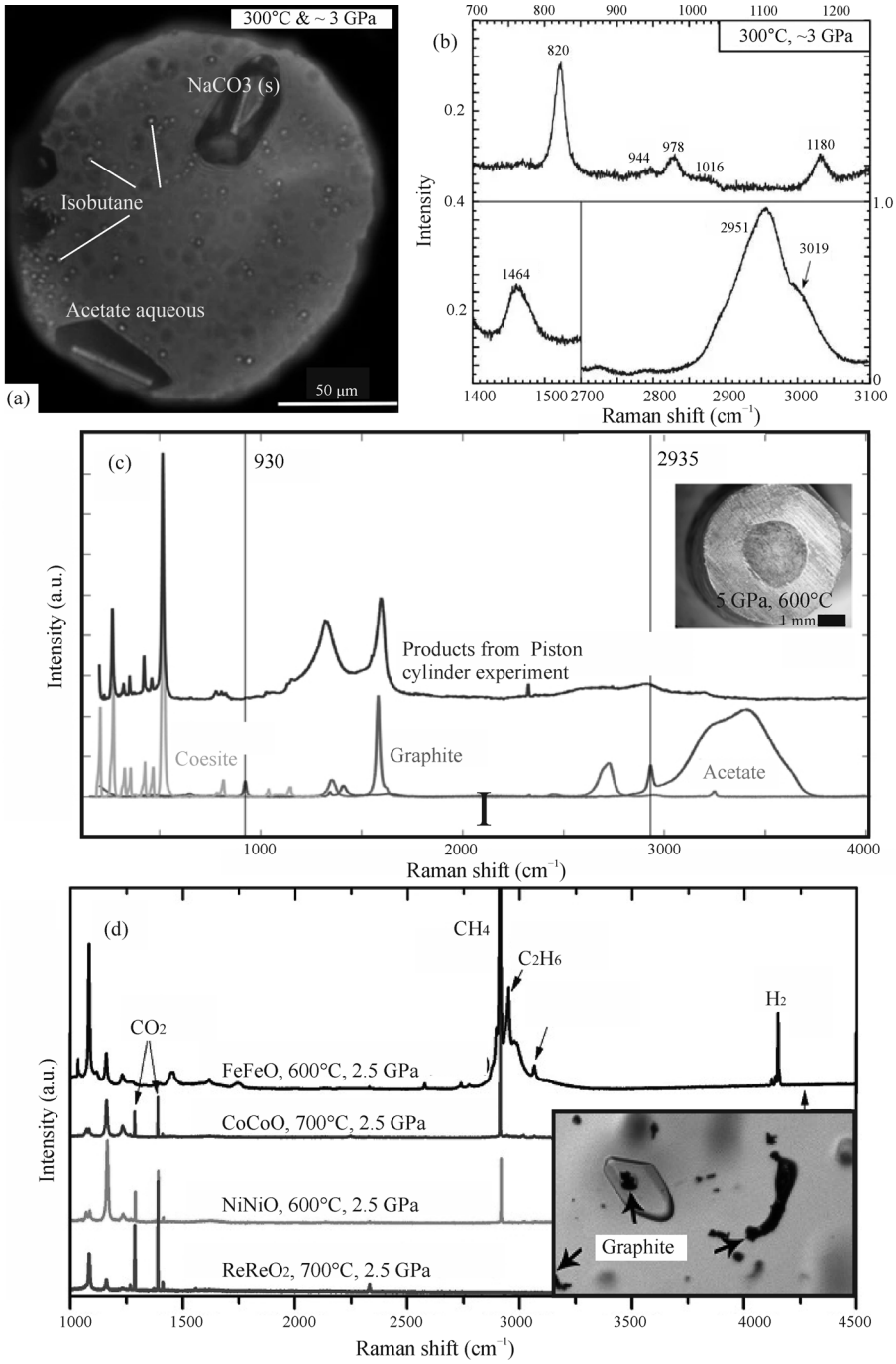

Fig. 9. The stability and speciation of organic compounds in high-pressure aqueous systems constrained by experimental simulations.
(a–b) Aqueous fluid, droplets of hydrocarbon fluid, and Na‐carbonate crystals after heating aqueous sodium acetate solution (CH_3COONa, 1.0 molal) at 3 GPa and 300°C, and (b) corresponding Raman spectra of a droplet of hydrocarbon fluid (modified after Huang et al., 2017); (c) Raman spectra of the product after reaction of aqueous sodium acetate solution (purple) at 5 GPa and 600°C by piston-cylinder experiments (modified after Szlachta et al., 2022). Reference spectra of the initial acetate solution (blue), of graphite (orange) and of coesite (yellow) are shown for comparison. Neither the 930 cm^{-1} nor the 2935 cm^{-1} band of acetate can be detected in the run products. The inset shows the opened silver capsule with the charge and the gray discoloration due to a carbonaceous material formed by the decomposition of the acetate; (d) representative Raman spectra of synthetic fluid inclusions in quartz formed from formic acid solution at 2.5 GPa, 600–700°C, and fO_2 buffered by the Fe–FeO to the Re–ReO_2 buffer (modified after Li, 2017). Note that the gas species vary as a function of fO_2. The inset shows graphite occurs in fluid inclusions and also as solid inclusions in quartz (experimental conditions: 2.5 GPa, 600°C, NNO–fO_2 buffer).

transitions, as depicted in our flow chart (Fig. 10), which remain a wide, active, and challenging frontier for future research. Systematic research needs to be carried out, especially to match thermodynamics predictions and high *P-T* experiments with real geological environments. In the following, we highlight specific future avenues for advancement in this field.

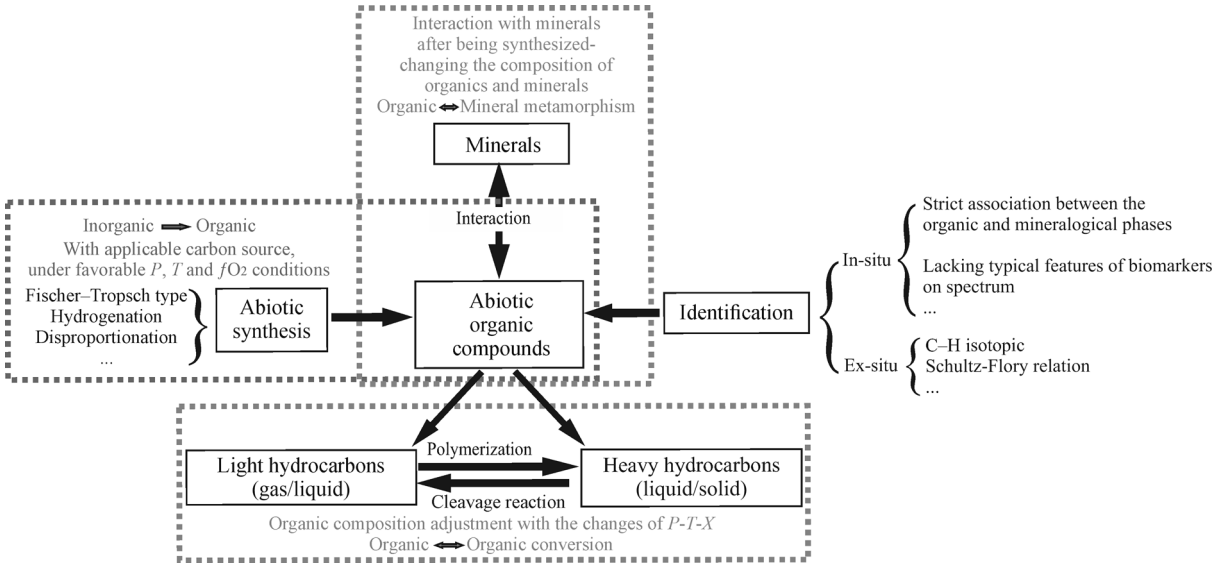

Fig. 10. Flow chart of research on abiotic organic matter on Earth.

5.1 Exploring the diversity of abiotic organic compound formation pathways

In petrologic studies, the production of abiotic organics has largely focused on serpentinization, as significant H_2 production and reaction to form abiotic organic molecules is known to occur from natural observation, experimental simulations, and thermodynamic predictions in crustal hydrothermal systems. However, abiotic organic compounds, mainly CH_4, have also been reported in metabasalts, alkaline magmatic rocks, and ultradeep diamonds, and such compounds may be prevalent in other as-yet-undiscovered environments. The experimental synthesis also demonstrates additional pathways for the formation of abiotic organic compounds, such as carbonate hydrogenation reactions and disproportionation reactions of siderite in water; However, the investigated *P-T-*fO_2 range remains limited. For example, many experiments are conducted at conditions far from those of the deep mantle or the real subduction zone geothermal gradient. The proposed chemical reactions could be investigated with modern experimental techniques coupled with in situ characterization methods, e.g., Raman, FTIR, and XRD, over more realistic *P-T* conditions. Additionally, in many experiments the reactants do not represent natural mineral composition in the deep Earth. For example, Fe^0 or FeO are often used as reactants, whereas the redox conditions for FeO–Fe metal saturation do not occur at depths ≤ 250 km (Rohrbach and Schmidt, 2011). Instead, minerals containing Fe^{2+}–Fe^{3+} are the main reactants involved in natural systems. Another example are experiments with $CaCO_3$ at pressures greater than 10 GPa, as subducted Ca-carbonates will react with silicate minerals to produce Mg-carbonates during HP metamorphism. Future high *P-T* experiments can be guided by natural observations, such as CH_4–H_2 in some silicate-melt inclusions or metallic-melt inclusions in the deep lower-mantle. As a result, experiments should not be limited to water-rock or gas-liquid systems, an area which is little explored.

5.2 Exploring the diversity of abiotic organic compounds under high-pressure

Methane is the most commonly observed abiotic organic molecule and the diversity of other possible compounds deep Earth remains largely undiscovered.

(1) Do more organic molecules exist in the deep Earth?

The formation mechanisms for heavier hydrocarbons remain controversial and unexplored. During the first step of synthesis (inorganic → organic), the different reactants used in experiments appear to result in the production of different organic species. From the limited experimental data, we speculate that serpentine and siderite are favorable reactants for the formation of unsaturated hydrocarbons. In addition, the transformation from one abiotic organic molecule to another (organic ↔ organic) has been an important focus for organic chemists and material scientists, laying the foundation for geological studies of organic ↔ organic phase transitions. For example, experiments confirm that CH_4 can polymerize to form higher hydrocarbons under extremely high-temperature conditions (>1500 K), but analogous to the experimental results of organic chemists, the macromolecular organics can be more easily formed via polycondensation of unsaturated hydrocarbons, e.g., alkene (< 1000 K). Such a process may be more consistent with the *P-T* conditions of subduction. Water is perhaps the most important compound in subduction zones, driving or playing a major role in most tectonometamorphic, seismic, and volcanic processes. Water is also an important reactant for the generation of HCs, and the formation of these compounds may therefore be tied to a range of other deep water-driven geologic processes. Some pioneering work has already been carried out, such as the studies of Sharma et al. (2009), Huang et al. (2017), Li Y. (2017), and Szlachta et al. (2022), which demonstrate that the polymerization or decomposition process of organics will become more active and complex under water-rich conditions. Systematic investigation of

organic ↔ organic reactions in complex systems (e.g., water-participated reactions), in both natural rock systems and high *P-T* experiments, is an exciting avenue for future research.

(2) Do rock-hosted solid organic compounds occur in nature?

Solid carbon compounds are an important host for carbon in marine serpentinites. Could such solid organic compounds represent an important, but largely unconstrained, fraction of carbon in the deep earth?

At this time, very few natural occurrences of solid organic compounds in HP metamorphic rocks have been discovered. Debret et al. (2022) have found such compounds in subducted serpentinite, but at pressures of <0.6 GPa. Experiments show that organic compounds, i.e., CCM, with a high C: H ratio can survive extreme *P-T* conditions; However, such compounds are difficult to identify by commonly used Raman or IR spectrometers. Therefore, specialized and highly sensitive characterization techniques are required to identify the chemical bonds formed between rare heteroatoms and carbon in their original context, as the molecular structure can be destroyed and context is lost by dissolution methods (for the GC measurement).

In the field of experimental petrology, most studies have focused on the synthesis of organic molecules in their fluid or gaseous state. Minerals can be used as (1) experimental reactants, such as olivine to produce H_2, (2) redox buffers, such as hematite–magnetite (HM), fayalite–quartz–magnetite (FMQ) assemblages, and (3) as a potential catalyst for organic reactions (Andreani and Ménez, 2019). Rarely are these phases carefully characterized after the experiment to determine if CCM is produced as an independent phase or adsorbed onto mineral surfaces (Andreani and Ménez, 2019). Such interactions between organic molecules and minerals can contribute to the redox conditions of the deep earth, as well as playing a role in generating compounds that might have contributed to the origin of life and deep energy sources, that is, when these solids migrate from deeper environments to the surface other organic components can be released (Yabuta et al., 2007; Pizzarello et al., 2010).

5.3 Approaches to understanding abiotic organic synthesis based on comparative planetology

From the detection of complex organics in solar system objects, stars, and galaxies, we know that complex organics are synthesized abiotically on a large scale and occur in many planetary to interstellar environments. First, these environments can act as analogues to those in the early Earth or the future Earth. For example, haze-induced photochemical reactions involving organics take place on Neptune and might have occurred in early Earth before a stable atmosphere had formed. Such processes could have contributed nutrients to the 'prebiotic soup' that supports life through substance cycles between the atmosphere and surface. Additionally, mineralogical and petrological studies of carbonaceous chondrites may help identify processes that formed early abiotic amino acids. Furthermore, thermodynamics models, high *P-T* experiments, and other techniques used to study terrestrial processes can be applied to extraterrestrial environments.

Given the widespread existence of abiotic organic matter across the Universe, one can ask what makes Earth so unique in terms of the development of life. Unlike other objects in our solar system, most organic molecules on Earth are derived from biological activity (Kwok, 2017). Therefore, there must have been additional factors, such as the development of a stable atmosphere and magnetosphere, distance from the Earth to the sun, prevalence of liquid water, and tectonic activity, which produced the conditions from which simple abiotic organic matter could transition into life. Indeed, comparative planetary studies have contributed to our understanding of Earth's habitability and will continue to contribute in the future.

While Earth is now largely dominated by biotic organic compounds, the early Earth may have been different. The most well-known proponent of the existence of primordial hydrocarbons on Earth was Tommy Gold (1920–2004) (e.g., Bondi, 2006); Gold hypothesized that complex organics were synthesized from primordial CH_4 in the Earth's deep interior, which might have flowed to the surface to produce coal and oil (Gold, 1999; Kwok, 2017). Even in the present, the degree to which hydrocarbons on Earth are abiotic is only beginning to be recognized and may represent a larger fraction of organics than previously assumed. If Gold's (1999) hypothesis of abiogenic petroleum is true, other planets, besides Earth, would be the best natural laboratories to look for such processes. Future space exploration will answer these questions and provide numerous opportunities to advance our understanding of reduced volatile compounds and organic evolution on planetary bodies.

Acknowledgments

This work was financially supported by the National Key Research and Development Program of China (Grant No. 2019YFA0708501) and the NSFC Major Research Plan on West-Pacific Earth System Multispheric Interactions (Grant No. 92158206). Many thanks are due to the reviewers and Associate Editor for their careful editorial handling and helpful suggestions; Dr. Susan Turner (Brisbane) assisted with the final manuscript. Thanks are extended to the editorial office of Acta Geologica Sinica for the invitation to write a review paper on this topic for the occasion of the 100th Anniversary of the Geological Society of China and Acta Geologica Sinica.

Manuscript received Oct. 31, 2022
accepted Jan. 17, 2023
associate EIC: ZHANG Lifei
edited by GUO Xianqing

References

Andreani, M., and Ménez, B., 2019. New perspectives on abiotic organic synthesis and processing during hydrothermal alteration of the oceanic lithosphere. In: Orcutt, B., Daniel, I., and Dasgupta, R. (eds.), Deep Carbon: Past to Present. Cambridge: Cambridge University Press, 447–479.

Aoki, K., Kakudate, Y., Yoshida, M., Usuba, S., Tanaka, K., and Fujiwara, S., 1989. Solid-state polymerization of acetylene under pressure. Synthetic Metals, 28(3): D91–D98.

Berndt, M.E., Allen, D.E., and Seyfried, W.E. Jr., 1996.

Reduction of CO_2 during serpentinization of olivine at 300℃ and 500 bar. Geology, 24(4): 351–354.
Berry, A.J., and O'Neill, H.S.C., 2021. Oxygen content, oxygen fugacity, the oxidation state of iron, and mid-ocean ridge basalts. In: Moretti, R., and Neuville, D.R. (eds.), Magma Redox Geochemistry. Geophysical Monograph Series, American Geophysical Union, 155–163.
Block, S., Weir, C.E., and Piermarini, G.J., 1970. Polymorphism in benzene, naphthalene, and anthracene at high pressure. Science, 169(3945): 586–587.
Bondi, H., 2006. Thomas Gold 22 May 1920–22 June 2004. Biographical Memoirs of Fellows of the Royal Society, 52: 117–135.
Boutier, A., Brovarone, A.V., Martinez, I., Sissmann, O., and Mana, S., 2021. High-pressure serpentinization and abiotic methane formation in metaperidotite from the Appalachian subduction, northern Vermont. Lithos, 396: 106190.
Brovarone, A.V., Martinez, I., Elmaleh, A., Compagnoni, R., Chaduteau, C., Ferraris, C., and Esteve, I., 2017. Massive production of abiotic methane during subduction evidenced in metamorphosed ophicarbonates from the Italian Alps. Nature Communications, 8(1): 1–13.
Brovarone, A.V., Sverjensky, D.A., Piccoli, F., Ressico, F., Giovannelli, D., and Daniel, I., 2020. Subduction hides high-pressure sources of energy that may feed the deep subsurface biosphere. Nature Communications, 11(1): 1–11.
Busemann, H., Young, A.F., Alexander, C.M.O.D., Hoppe, P., Mukhopadhyay, S., and Nittler, L.R., 2006. Interstellar chemistry recorded in organic matter from primitive meteorites. Science, 312(5774): 727–730.
Chanyshev, A.D., Litasov, K.D., Shatskiy, A.F., Furukawa, Y., Yoshino, T., and Ohtani, E., 2015. Oligomerization and carbonization of polycyclic aromatic hydrocarbons at high pressure and temperature. Carbon, 84: 225–235.
Charlou, J.L., Donval, J.P., Fouquet, Y., Jean-Baptiste, P., and Holm, N., 2002. Geochemistry of high H_2 and CH_4 vent fluids issuing from ultramafic rocks at the Rainbow hydrothermal field (36°14′N, MAR). Chemical Geology, 191(4): 345–359.
Chekalyuk, E.B., 1971. Thermodynamic fundamentals of the theory of mineral genesis of oil. Naukova Dumka.
Chelazzi, D., Ceppatelli, M., Santoro, M., Bini, R., and Schettino, V., 2004. High-pressure synthesis of crystalline polyethylene using optical catalysis. Nature Materials, 3(7): 470–475.
Chen, J.Y., Jin, L.J., Dong, J.P., Zheng, H.F., and Liu, G.Y., 2008. Methane formation from $CaCO_3$ reduction catalyzed by high pressure. Chinese Chemical Letters, 19(4): 475–478.
Chiodini, G., 2009. CO_2/CH_4 ratio in fumaroles a powerful tool to detect magma degassing episodes at quiescent volcanoes. Geophysical Research Letters, 36: L02302.
Ciabini, L., Santoro, M., Gorelli, F.A., Bini, R., Schettino, V., and Raugei, S., 2007. Triggering dynamics of the high-pressure benzene amorphization. Nature materials, 6(1): 39–43.
Citroni, M., Ceppatelli, M., Bini, R., and Schettino, V., 2005. High-pressure reactivity of propene. The Journal of Chemical Physics, 123(19): 194510.
Cody, G.D., Heying, E., Alexander, C.M., Nittler, L.R., Kilcoyne, A.D., Sandford, S.A., and Stroud, R.M., 2011. Establishing a molecular relationship between chondritic and cometary organic solids. Proceedings of the National Academy of Sciences, 108(48): 19171–19176.
Connolly, J.A., 2005. Computation of phase equilibria by linear programming: A tool for geodynamic modeling and its application to subduction zone decarbonation. Earth and Planetary Science Letters, 236(1–2): 524–541.
Connolly, J.A., and Galvez, M.E., 2018. Electrolytic fluid speciation by Gibbs energy minimization and implications for subduction zone mass transfer. Earth and Planetary Science Letters, 501: 90–102.
Cottrell, E., Birner, S.K., Brounce, M., Davis, F.A., Waters, L.E., and Kelley, K.A., 2021. Oxygen fugacity across tectonic settings. In: Moretti, R., and Neuville, D.R. (eds.), Magma Redox Geochemistry. Geophysical Monograph Series, American Geophysical Union, 33–61.
Debret, B., Ménez, B., Walter, B., Bouquerel, H., Bouilhol, P., Mattielli, N., Pisapia C, Rigaudier T., and Williams, H.M., 2022. High-pressure synthesis and storage of solid organic compounds in active subduction zones. Science Advances, 8 (37): eabo2397.
Dischler, B., Bubenzer, A., and Koidl, P., 1983. Bonding in hydrogenated hard carbon studied by optical spectroscopy. Solid State Communications, 48(2): 105–108.
Eigenbrode, J.L., Summons, R.E., Steele, A., Freissinet, C., Millan, M., Navarro-González, R., and Coll, P., 2018. Organic matter preserved in 3-billion-year-old mudstones at Gale crater, Mars. Science, 360(6393): 1096–1101.
Etiope, G., and Sherwood Lollar, B., 2013. Abiotic methane on Earth. Reviews of Geophysics, 51(2): 276–299.
Evans, K.A., 2006. Redox decoupling and redox budgets: Conceptual tools for the study of earth systems. Geology, 34 (6): 489–492.
Fray, N., Bardyn, A., Cottin, H., Altwegg, K., Baklouti, D., Briois, C., and Hilchenbach, M., 2016. High-molecular-weight organic matter in the particles of comet 67P/ Churyumov–Gerasimenko. Nature, 538(7623): 72–74.
Frezzotti, M.L., 2019. Diamond growth from organic compounds in hydrous fluids deep within the Earth. Nature Communications, 10(1): 1–8.
Fu, B., Touret, J.L., Zheng, Y.F., and Jahn, B.M., 2003. Fluid inclusions in granulites, granulitized eclogites and garnet clinopyroxenites from the Dabie–Sulu terranes, eastern China. Lithos, 70(3–4): 293–319.
Garanin, V.K., Biller, A.Y., Skvortsova, V.L., Bovkun, A.V., and Bondarenko, G.V., 2011. Polyphase hydrocarbon inclusions in garnet from the Mir diamondiferous pipe. Moscow University Geology Bulletin, 66(2): 116–125.
Giardini, A.A., and Salotti, C.A., 1969. Kinetics and relations in the calcite-hydrogen reaction and relations in the dolomite-hydrogen and siderite-hydrogen systems. American Mineralogist: Journal of Earth and Planetary Materials, 54(7–8): 1151–1172.
Giardini, A.A., Salotti, C.A., and Lakner, J.F., 1968. Synthesis of graphite and hydrocarbons by reaction between calcite and hydrogen. Science, 159(3812): 317–319.
Glein, C.R., and Zolotov, M.Y., 2020. Hydrogen, hydrocarbons, and habitability across the solar system. Elements, 16(1): 47–52.
Goesmann, F., Rosenbauer, H., Bredehöft, J.H., Cabane, M., Ehrenfreund, P., Gautier, T., and Ulamec, S., 2015. Organic compounds on comet 67P/Churyumov-Gerasimenko revealed by COSAC mass spectrometry. Science, 349(6247): aab0689.
Gold, T., 1999. The Deep Hot Biosphere. New York: Springer, 11–36.
Hayes, J.M., 1967. Organic constituents of meteorites—A review. Geochimica et Cosmochimica Acta, 31(9): 1395–1440.
Holland, G., Lollar, B.S., Li, L., Lacrampe-Couloume, G., Slater, G.F., and Ballentine, C.J., 2013. Deep fracture fluids isolated in the crust since the Precambrian era. Nature, 497(7449): 357–360.
Holland, T., and Powell, R., 1991. A Compensated-Redlich-Kwong (CORK) equation for volumes and fugacities of CO_2 and H_2O in the range 1 bar to 50 kbar and 100–1600°C. Contributions to Mineralogy and Petrology, 109(2): 265–273.
Holland, T., and Powell, R., 2011. An improved and extended internally consistent thermodynamic dataset for phases of petrological interest, involving a new equation of state for solids. Journal of Metamorphic Geology, 29(3): 333–383.
Huang, F., Daniel, I., Cardon, H., Montagnac, G., and Sverjensky, D.A., 2017. Immiscible hydrocarbon fluids in the deep carbon cycle. Nature Communications, 8(1): 1–8.
Huang, J.X., Xiong, Q., Gain, S.E., Griffin, W.L., Murphy, T.D., Shiryaev, A.A., and O'Reilly, S.Y., 2020. Immiscible metallic melts in the deep Earth: clues from moissanite (SiC) in volcanic rocks. Science Bulletin, 65(17): 1479–1488.
Ildefonse, B., Blackman, D.K., John, B.E., Ohara, Y., Miller, D.J., and MacLeod, C.J., 2007. Oceanic core complexes and crustal accretion at slow-spreading ridges. Geology, 35(7): 623–626.
Kelley, D.S., 1996. Methane‐rich fluids in the oceanic crust.

Journal of Geophysical Research: Solid Earth, 101(B2): 2943–2962.
Kelley, D.S., Karson, J.A., Fruh-Green, G.L., Yoerger, D.R., Shank, T.M., Butterfield, D.A., and Sylva, S.P., 2005. A serpentinite-hosted ecosystem: the Lost City hydrothermal field. Science, 307(5714): 1428–1434.
Kenney, J.F., Kutcherov, V.A., Bendeliani, N.A., and Alekseev, V.A., 2002. The evolution of multicomponent systems at high pressures: VI. The thermodynamic stability of the hydrogen–carbon system: The genesis of hydrocarbons and the origin of petroleum. Proceedings of the National Academy of Sciences, 99(17): 10976–10981.
Kim, S.J., Jung, A., Sim, C.K., Courtin, R., Bellucci, A., Sicardy, B.,Song, I.O., and Minh, Y.C., 2011. Retrieval and tentative indentification of the 3 μm spectral feature in Titan's haze. Planetary and Space Science, 59(8): 699–704.
Klein, F., Tarnas, J.D., and Bach, W., 2020. Abiotic sources of molecular hydrogen on Earth. Elements, 16(1): 19–24.
Kutcherov, V.G., and Krayushkin, V.A., 2010. Deep‐seated abiogenic origin of petroleum: From geological assessment to physical theory. Reviews of Geophysics, 48(1): RG1001.
Kutcherov, V.G., Bendeliani, N.A., Alekseev, V.A., and Kenney, J.F., 2002. Synthesis of hydrocarbons from minerals at pressures up to 5 GPa. Doklady Physical Chemistry. Kluwer Academic Publishers-Plenum Publishers, 387(4): 328–331.
Kwok, S., 2004. The synthesis of organic and inorganic compounds in evolved stars. Nature, 430(7003): 985–991.
Kwok, S., 2009. Organic matter in space: From star dust to the Solar System. Astrophysics and Space Science, 319(1): 5–21.
Kwok, S., 2015. Organic compounds in circumstellar and interstellar environments. Origins of Life and Evolution of Biospheres, 45(1): 113–121.
Kwok, S., 2017. Abiotic synthesis of complex organics in the universe. Nature Astronomy, 1(10): 642–643.
Kwok, S., 2019. Organics in the solar system. Research in Astronomy and Astrophysics, 19(4): 049.
Kwok, S., and Zhang, Y., 2011. Mixed aromatic-aliphatic organic nanoparticles as carriers of unidentified infrared emission features. Nature, 479(7371): 80–83.
Kwok, S., and Zhang, Y., 2013. Unidentified infrared emission bands: PAHs or MAONs? The Astrophysical Journal, 771(1): 5.
Le Gall, A., Malaska, M.J., Lorenz, R.D., Janssen, M.A., Tokano, T., Hayes, A.G., Mastrogiuseppe, M., Lunine, J.I., Veyssière, G., Encrenaz, P., and Karatekin, O., 2016. Composition, seasonal change, and bathymetry of Ligeia Mare, Titan, derived from its microwave thermal emission. Journal of Geophysical Research: Planets, 121(2): 233–251.
Le, T., Striolo, A., Turner, C.H., and Cole, D.R., 2017. Confinement effects on carbon dioxide methanation: A novel mechanism for abiotic methane formation. Scientific Reports, 7(1): 1–12.
Li, Y., 2017. Immiscible CHO fluids formed at subduction zone conditions. Geochemical Perspectives Letters, 3: 12–21.
Lobanov, S.S., Chen, P.N., Chen, X.J., Zha, C.S., Litasov, K.D., Mao, H.K., and Goncharov, A.F., 2013. Carbon precipitation from heavy hydrocarbon fluid in deep planetary interiors. Nature Communications, 4(1): 1–8.
Marocchi, M., Bureau, H., Fiquet, G., and Guyot, F., 2011. In-situ monitoring of the formation of carbon compounds during the dissolution of iron (II) carbonate (siderite). Chemical Geology, 290(3–4): 145–155.
McCollom, T.M., 2003. Formation of meteorite hydrocarbons from thermal decomposition of siderite ($FeCO_3$). Geochimica et Cosmochimica Acta, 67(2): 311–317.
McCollom, T.M., 2016. Abiotic methane formation during experimental serpentinization of olivine. Proceedings of the National Academy of Sciences, 113(49): 13965–13970.
McCollom, T.M., and Seewald, J.S., 2006. Carbon isotope composition of organic compounds produced by abiotic synthesis under hydrothermal conditions. Earth and Planetary Science Letters, 243(1–2): 74–84.
McCollom, T.M., and Seewald, J.S., 2007. Abiotic synthesis of organic compounds in deep-sea hydrothermal environments. Chemical Reviews, 107(2): 382–401.
McCollom, T.M., Ritter, G., and Simoneit, B.R., 1999. Lipid synthesis under hydrothermal conditions by Fischer-Tropsch-type reactions. Origins of Life and Evolution of the Biosphere, 29(2): 153–166.
McSween, H.Y.Jr., 1979. Are carbonaceous chondrites primitive or processed? A review. Reviews of Geophysics, 17(5): 1059–1078.
Mendeleev, D., 1877. L'Origine du pétrole, Second series, vol. VIII, Revue Scientifique, 409–416.
Ménez, B., 2020. Abiotic hydrogen and methane: Fuels for life. Elements, 16(1): 39–46.
Ménez, B., Pasini, V., and Brunelli, D., 2012. Life in the hydrated suboceanic mantle. Nature Geoscience, 5(2): 133–137.
Ménez, B., Pasini, V., Guyot, F., Benzerara, K., Bernard, S., and Brunelli, D., 2018a. Mineralizations and transition metal mobility driven by organic carbon during low-temperature serpentinization. Lithos, 323: 262–276.
Ménez, B., Pisapia, C., Andreani, M., Jamme, F., Vanbellingen, Q.P., Brunelle, A., Richard, L., Dumas, P., and Réfrégiers, M., 2018b. Abiotic synthesis of amino acids in the recesses of the oceanic lithosphere. Nature, 564(7734): 59–63.
Mével, C., 2003. Serpentinization of abyssal peridotites at mid-ocean ridges. Comptes Rendus Geoscience, 335(10–11): 825–852.
Milesi, V., McCollom, T. M., and Guyot, F., 2016. Thermodynamic constraints on the formation of condensed carbon from serpentinization fluids. Geochimica et Cosmochimica Acta, 189: 391–403.
Mukherjee, B.K., and Sachan, H.K., 2009. Fluids in coesite-bearing rocks of the Tso Morari Complex, NW Himalaya: Evidence for entrapment during peak metamorphism and subsequent uplift. Geological Magazine, 146(6): 876–889.
Mukhina, E., Kolesnikov, A., and Kutcherov, V., 2017. The lower *P-T* limit of deep hydrocarbon synthesis by $CaCO_3$ aqueous reduction. Scientific Reports, 7(1): 1–5.
Nan, J., King, H.E., Delen, G., Meirer, F., Weckhuysen, B.M., Guo, Z., Peng, X.T., and Plümper, O., 2021. The nanogeochemistry of abiotic carbonaceous matter in serpentinites from the Yap Trench, western Pacific Ocean. Geology, 49(3): 330–334.
Naraoka, H., 2014. Insoluble Organic Matter. In: Gargaud, M., Amils, R., Quintanilla, J.C., Cleaves, H.J., Irvine, W.M., Pinti, D.L., and Viso, M. (eds.), Encyclopedia of Astrobiology. Berlin: Springer, 1–1853.
Peña-Alvarez, M., Brovarone, A.V., Donnelly, M.E., Wang, M., Dalladay-Simpson, P., Howie, R., and Gregoryanz, E., 2021. In-situ abiogenic methane synthesis from diamond and graphite under geologically relevant conditions. Nature Communications, 12(1): 1–5.
Peng, W., Zhang, L., Tumiati, S., Brovarone, A.V., Hu, H., Cai, Y., and Shen, T., 2021. Abiotic methane generation through reduction of serpentinite-hosted dolomite: Implications for carbon mobility in subduction zones. Geochimica et Cosmochimica Acta, 311: 119–140.
Pizzarello, S., and Shock, E., 2010. The organic composition of carbonaceous meteorites: The evolutionary story ahead of biochemistry. Cold Spring Harbor Perspectives in Biology, 2 (3): a002105.
Plümper, O., King, H.E., Geisler, T., Liu, Y., Pabst, S., Savov, I.P., Rost, D., and Zack, T., 2017. Subduction zone forearc serpentinites as incubators for deep microbial life. Proceedings of the National Academy of Sciences, 114(17): 4324–4329.
Postberg, F., Khawaja, N., Abel, B., Choblet, G., Glein, C.R., Gudipati, M.S., and Waite, J.H., 2018. Macromolecular organic compounds from the depths of Enceladus. Nature, 558 (7711): 564–568.
Potter, J., Rankin, A.H., and Treloar, P.J., 2004. Abiogenic Fischer–Tropsch synthesis of hydrocarbons in alkaline igneous rocks; fluid inclusion, textural and isotopic evidence from the Lovozero complex, NW Russia. Lithos, 75(3–4): 311–330.
Reeves, E.P., and Fiebig, J., 2020. Abiotic synthesis of methane and organic compounds in Earth's lithosphere. Elements, 16 (1): 25–31.

Reller, A., Padeste, C., and Hug, P., 1987. Formation of organic carbon compounds from metal carbonates. Nature, 329(6139): 527–529.
Rohrbach, A., and Schmidt, M.W, 2011. Redox freezing and melting in the Earth's deep mantle resulting from carbon–iron redox coupling. Nature, 472(7342): 209–212.
Saxena, S.K., and Fei, Y., 1987. High pressure and high temperature fluid fugacities. Geochimica et Cosmochimica Acta, 51(4): 783–791.
Scott, H.P., Hemley, R.J., Mao, H.K., Herschbach, D.R., Fried, L.E., Howard, W.M., and Bastea, S., 2004. Generation of methane in the Earth's mantle: In situ high pressure–temperature measurements of carbonate reduction. Proceedings of the National Academy of Sciences, 101(39): 14023–14026.
Seewald, J.S., Zolotov, M.Y., and McCollom, T., 2006. Experimental investigation of single carbon compounds under hydrothermal conditions. Geochimica et Cosmochimica Acta, 70(2): 446–460.
Sforna, M.C., Brunelli, D., Pisapia, C., Pasini, V., Malferrari, D., and Ménez, B., 2018. Abiotic formation of condensed carbonaceous matter in the hydrating oceanic crust. Nature Communications, 9(1): 1–8.
Sharma, A., Cody, G.D., and Hemley, R.J., 2009. In situ diamond-anvil cell observations of methanogenesis at high pressures and temperatures. Energy and Fuels, 23(11): 5571–5579.
Sherwood Lollar, B., Frape, S.K., Weise, S.M., Fritz, P., Macko, S.A., and Welhan, J.A., 1993. Abiogenic methanogenesis in crystalline rocks. Geochimica et Cosmochimica Acta, 57(23–24): 5087–5097.
Sherwood Lollar, B., Onstott, T.C., Lacrampe-Couloume, G., and Ballentine, C.J., 2014. The contribution of the Precambrian continental lithosphere to global H_2 production. Nature, 516(7531): 379–382.
Sherwood Lollar, B., Westgate, T.D., Ward, J.A., Slater, G.F., and Lacrampe-Couloume, G., 2002. Abiogenic formation of alkanes in the Earth's crust as a minor source for global hydrocarbon reservoirs. Nature, 416(6880): 522–524.
Smith, E.M., Shirey, S.B., Nestola, F., Bullock, E.S., Wang, J., Richardson, S.H., and Wang, W., 2016. Large gem diamonds from metallic liquid in Earth's deep mantle. Science, 354 (6318): 1403–1405.
Smith, E.M., Shirey, S.B., Richardson, S.H., Nestola, F., Bullock, E.S., Wang, J., and Wang, W., 2018. Blue boron-bearing diamonds from Earth's lower mantle. Nature, 560 (7716): 84–87.
Sverjensky, D., 2020. The changing character of Carbon in fluids with pressure: Organic geochemistry of Earth's upper mantle fluids. In: Manning, C.E., Lin, J., and Mao, W.L. (eds.), Carbon in Earth's Interior. Geophysical Monograph Series, Wiley, 259–269.
Sverjensky, D.A., Stagno, V., and Huang, F., 2014. Important role for organic carbon in subduction-zone fluids in the deep carbon cycle. Nature Geoscience, 7(12): 909–913.
Szlachta, V., Vlasov, K., and Keppler, H., 2022. On the stability of acetate in subduction zone fluids. Geochemical Perspectives Letters, 21: 28–31.
Tao, R., Zhang, L., Tian, M., Zhu, J., Liu, X., Liu, J., Höfer, H.E., Stagno, V., and Fei, Y., 2018. Formation of abiotic hydrocarbon from reduction of carbonate in subduction zones: Constraints from petrological observation and experimental simulation. Geochimica et Cosmochimica Acta, 239: 390–408.
Thompson, M.A., Krissansen-Totton, J., Wogan, N., Telus, M., and Fortney, J.J., 2022. The case and context for atmospheric methane as an exoplanet biosignature. Proceedings of the National Academy of Sciences, 119(14): e2117933119.
Tobie, G., Gautier, D., and Hersant, F., 2012. Titan's bulk composition constrained by Cassini-Huygens: Implication for internal outgassing. The Astrophysical Journal, 752(2): 125.
Truche, L., McCollom, T.M., and Martinez, I., 2020. Hydrogen and abiotic hydrocarbons: Molecules that change the world. Elements: An International Magazine of Mineralogy, Geochemistry, and Petrology, 16(1): 13–18.
Vacquand, C., Deville, E., Beaumont, V., Guyot, F., Sissmann, O., Pillot, D., and Prinzhofer, A., 2018. Reduced gas seepages in ophiolitic complexes: Evidences for multiple origins of the H_2-CH_4-N_2 gas mixtures. Geochimica et Cosmochimica Acta, 223: 437–461.
Walters, J.B., Cruz-Uribe, A.M., and Marschall, H.R., 2020. Sulfur loss from subducted altered oceanic crust and implications for mantle oxidation. Geochemical Perspectives Letters, 13: 36–41.
Wang, C., Ren, L.A., Walters, J.B., Zhang, L., and Tao, R., 2023. In situ Raman vibrational spectra of siderite ($FeCO_3$) and rhodochrosite ($MnCO_3$) up to 47 GPa and 1100 K. American Mineralogist, 108(2): 312–325.
Wang, C., Tao, R., Walters, J.B., Höfer, H.E., and Zhang, L., 2022. Favorable P-T-fO_2 conditions for abiotic CH_4 production in subducted oceanic crusts: A comparison between CH_4-bearing ultrahigh-and CO_2-bearing high-pressure eclogite. Geochimica et Cosmochimica Acta, 336: 269–290.
Weng, K., Wang, B., Xiao, W., Xu, S., Lu, G., and Zhang, H., 1999. Experimental study on hydrocarbon formation due to reactions between carbonates and water or water-bearing minerals in deep earth. Chinese Journal of Geochemistry, 18 (2): 115–120.
Wogan, N., Krissansen-Totton, J., and Catling, D.C., 2020. Abundant atmospheric methane from volcanism on terrestrial planets is unlikely and strengthens the case for methane as a biosignature. The Planetary Science Journal, 1(3): 58.
Yabuta, H., Williams, L.B., Cody, G.D., Alexander, C.M.O.D., and Pizzarello, S., 2007. The insoluble carbonaceous material of CM chondrites: A possible source of discrete organic compounds under hydrothermal conditions. Meteoritics and Planetary Science, 42(1): 37–48.
Yang, X., Li, Y., Wang, Y., Zheng, H., Li, K., and Mao, H.K., 2021. Chemical transformations of *n*-hexane and cyclohexane under the upper mantle conditions. Geoscience Frontiers, 12 (2): 1010–1017.
Zhang, C., and Duan, Z., 2009. A model for C–O–H fluid in the Earth's mantle. Geochimica et Cosmochimica Acta, 73(7): 2089–2102.
Zhang, L., Zhang, L., Tang, M., Wang, X., Tao, R., Xu, C., and Bader, T., 2023. Massive abiotic methane production in eclogite during cold subduction. National Science Review, 10 (1): nwac207.

About the first author

WANG Chao is a Ph.D. student in the School of Earth and Space Sciences at Peking University. His current research focuses on the abiotic generation of hydrocarbons in the Earth's deep interior, with emphasis on the application of thermodynamic simulations, high *P-T* experimental simulations, and in situ highly temporal/spatial-resolved spectroscopic petrological investigation techniques. His research interest is mainly in the field of high-pressure fluid-rock interactions, nano-geochemistry, and in situ high-pressure experimental technology, especially those related to deep carbon behaviors. E-mail: wangchao1996@pku.edu.cn.

About the corresponding author

ZHANG Lifei is a professor in the School of Earth and Space Sciences at Peking University. His research interest is mainly in the field of high-pressure and high-temperature metamorphism in the subduction zones, orogenic belt evolutions, and deep carbon cycle, with emphasis on the application of petrological investigations, numerical simulations, and experimental simulations. His current research focuses on the abiotic generation of hydrocarbons in subduction zones. E-mail: lfzhang@pku.edu.cn.